Pseudo-Nambu-Goldstone boson as thermal dark matter

Takashi Toma

Kashiwa dark matter symposium 2021 at virtual

Based on PRL 119 191801, JHEP 1812 (2018) 089,
PLB 822 (2021) 136639,
JHEP 05 (2020) 057, PRD 104 (2021) 3, 035011

Collaborators:
Christian Gross (Pisa), Koji Ishiwata (Kanazawa), Oleg Lebedev (Helsinki),
Yoshihiko Abe (Kyoto), Koji Tsumura (Kyushu) and more

Outline

Nature of DM

- Stable (at least longer than age of universe)
- Electrically neutral (may have very small charge)
- Occupy 27% of energy density of the universe
- Graviational interaction
- Non-relativistic (cold)

Strong candidates:
WIMP, FIMP, SIMP,
axion, sterile neutrino,
primodial black holes
etc ↑
Revived by recent observations of gravitational waves

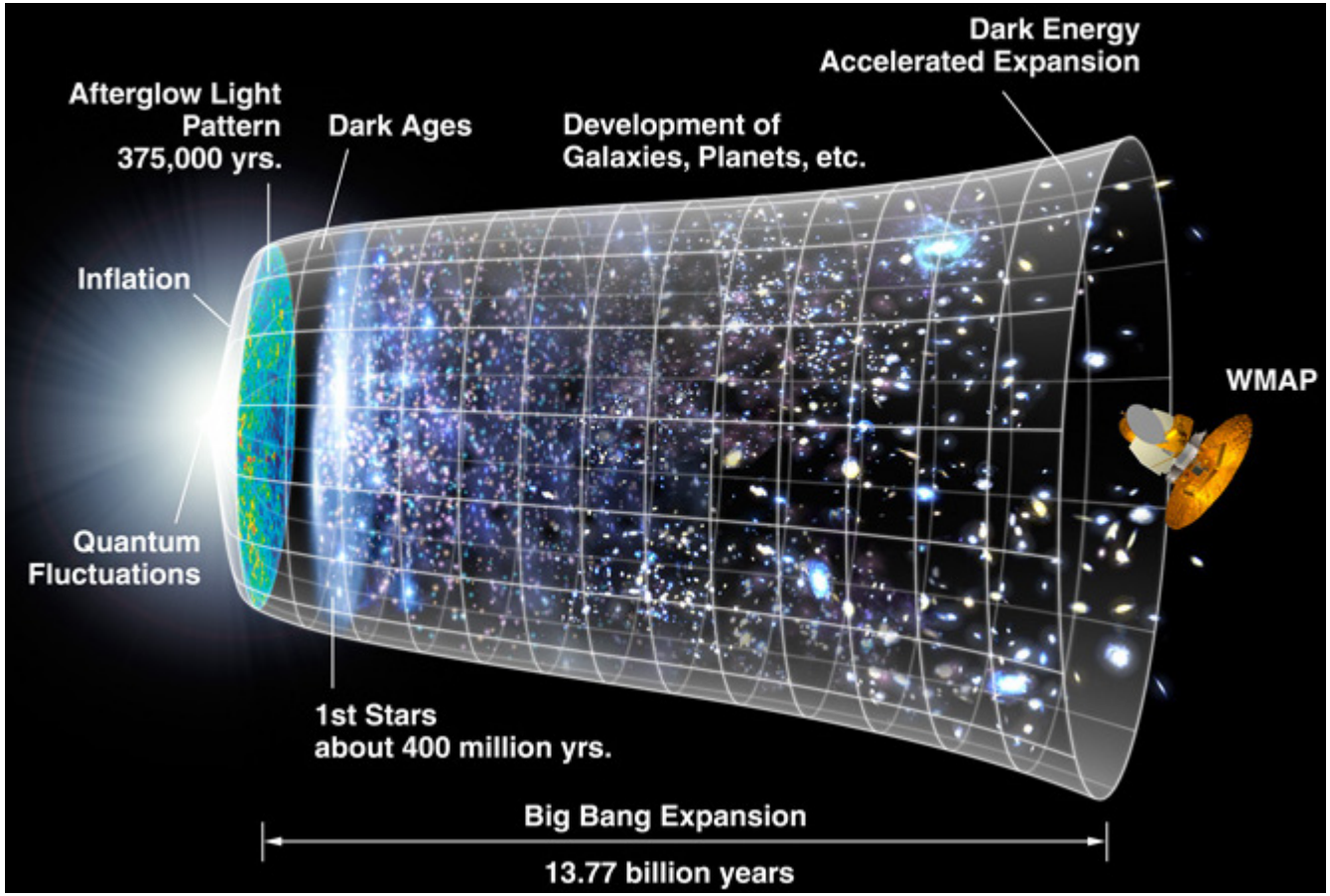

WIMP thermal production

Evolution of DM number density follows the Boltzmann eq.

$$\frac{dn_\chi}{dt} + 3Hn_\chi = -\langle\sigma v\rangle \left(n_\chi^2 - n_\chi^{\mathrm{eq}2}\right)$$

change variables $t \leftrightarrow x \equiv \dfrac{m}{T}, \quad n_\chi \leftrightarrow Y \equiv \dfrac{n_\chi}{s}, \qquad \Gamma \equiv \langle\sigma v\rangle\, n_\chi^{\mathrm{eq}},$

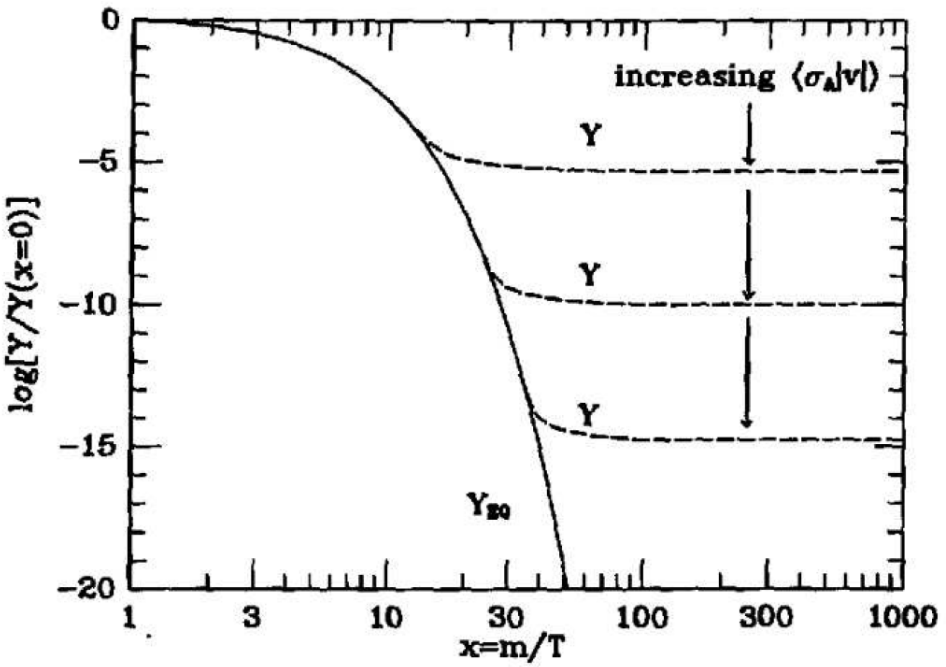

- DM relic is determined by $\langle\sigma v\rangle$.
- σv can be expanded by v.
  $\rightarrow \sigma v = a + bv^2 + \mathcal{O}\left(v^4\right)$
  a: s-wave, b: p-wave
- $\Omega h^2 \sim \dfrac{10^{-10}\ [\mathrm{GeV}^{-2}]}{\langle\sigma v\rangle} \sim 0.1$
  (Planck Coll.)
  $\rightarrow \langle\sigma v\rangle \sim 10^{-9}\ [\mathrm{GeV}^{-2}]$
  $\approx 10^{-26}\ [\mathrm{cm}^3/\mathrm{s}]$

WIMP search status

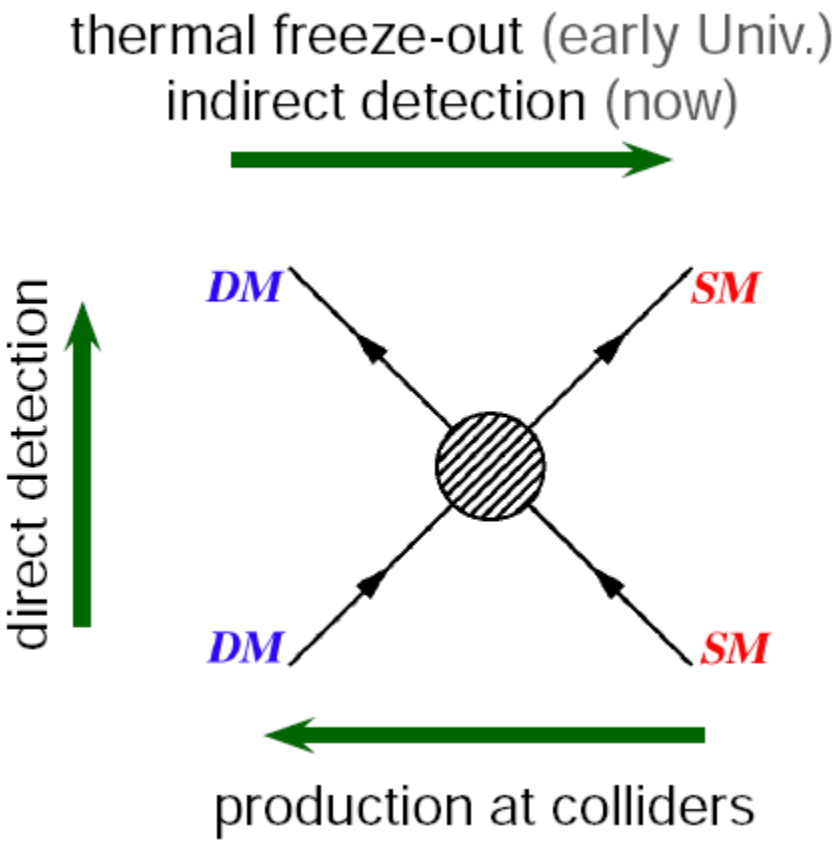

Collider search

Summary plot from ATLAS

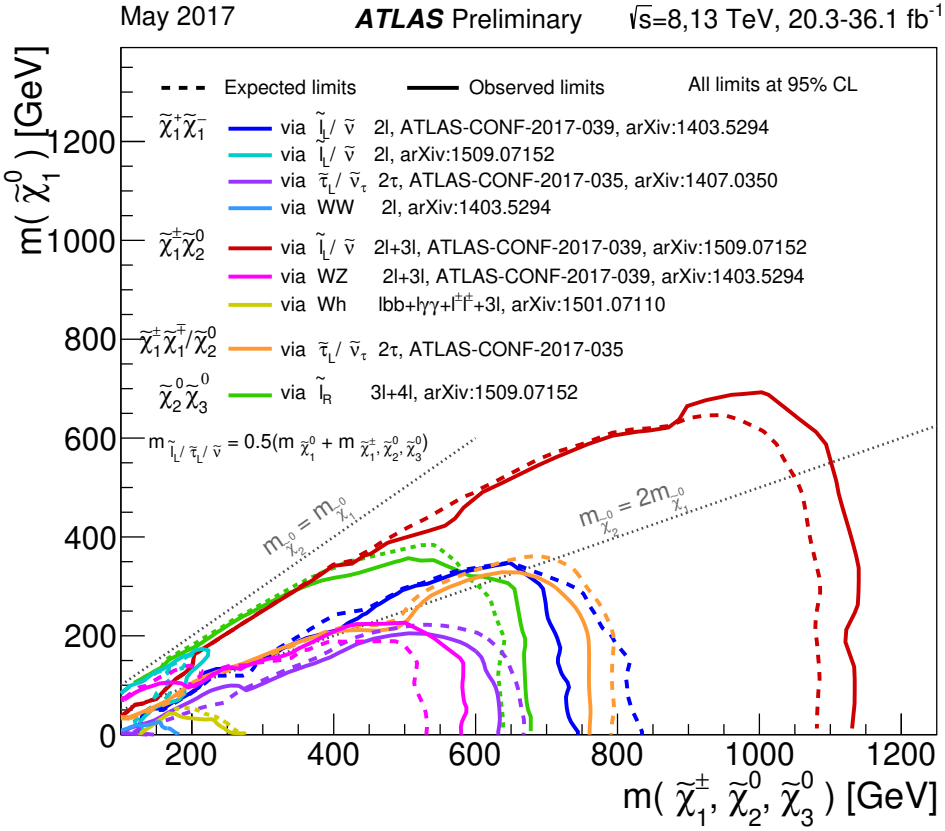

- WIMP DM can experimentally be detectable.
- Collider search: mass degenerate is required.

WIMP search status

Direct detection

PandaX-4T (2021) 2107.13438

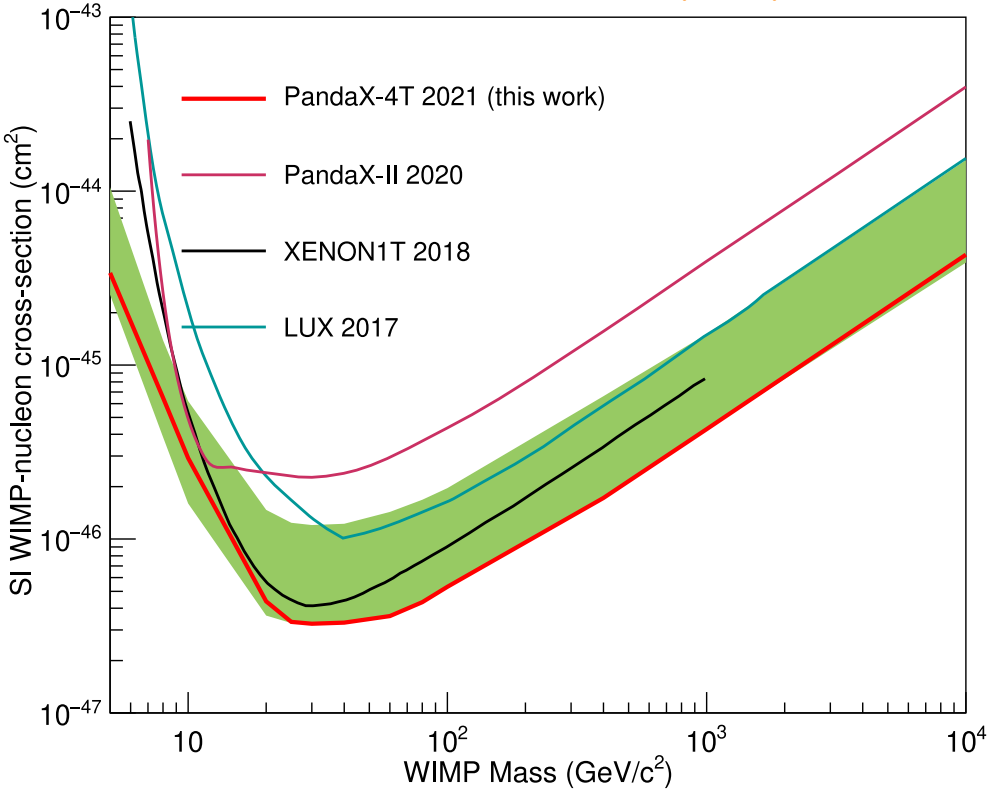

XENON1T (2020)

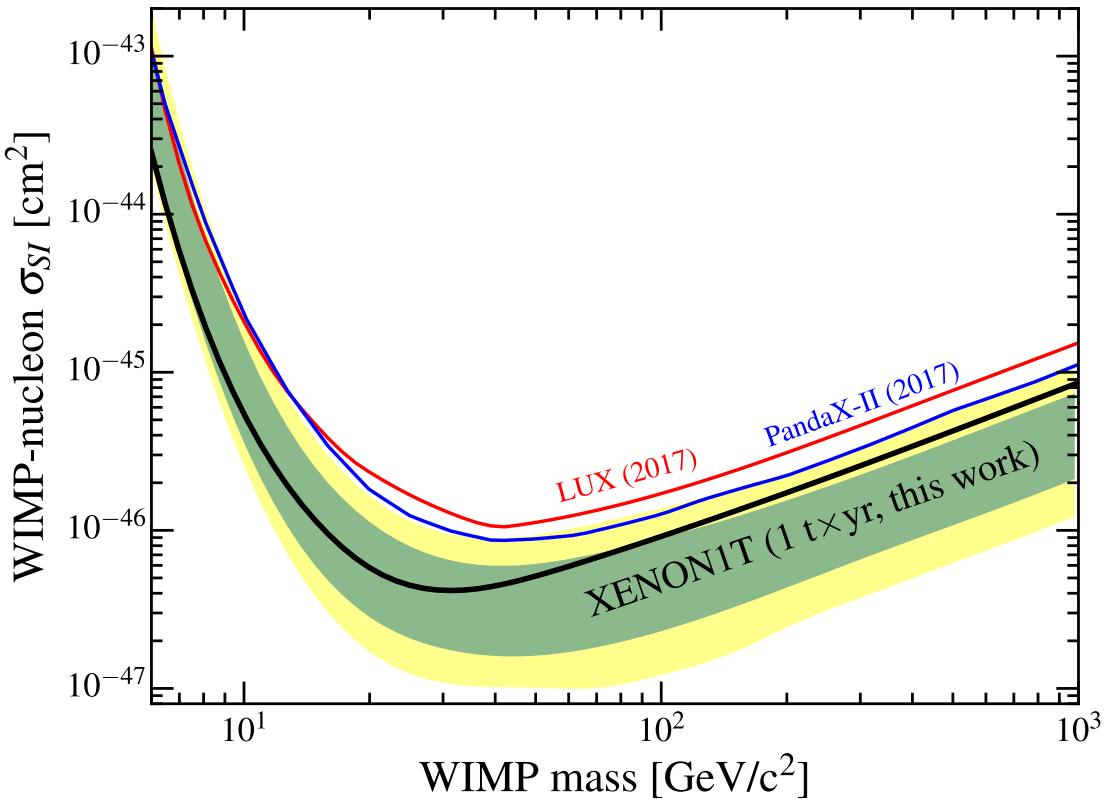

- Experimental bounds are stronger and stronger.
- Interactions between DM and SM are very weak? $\rightarrow$ non-WIMP DM?

In this talk, I will consider a simple DM model naturally evading the strong DD constraint. $\Rightarrow$ pseudo-Nambu-Goldstone boson

Pseudo-Nambu-Goldstone DM

PNGB DM model

C. Gross, O. Lebedev, TT, PRL (2017) [arXiv:1708.02253]

- Introduce complex scalar field $S = (s + i\chi)/\sqrt{2}$
- Global $U(1)$ symmetry is assumed (invariant under $S \to e^{i\alpha} S$)

$$\mathcal{V} = -\frac{\mu_H^2}{2}|H|^2 - \frac{\mu_S^2}{2}|S|^2 + \frac{\lambda_H}{2}|H|^4 + \lambda_{HS}|H|^2|S|^2 + \frac{\lambda_S}{2}|S|^4 - \left(\frac{\mu_S'^2}{4}S^2 + \text{H.c.}\right) \quad \leftarrow \text{soft breaking mass term}$$

- After H and S get VEVs, ϕ and s mix

$$H = \begin{pmatrix} 0 \\ (v+\phi)/\sqrt{2} \end{pmatrix}, \qquad S = \frac{v_s + s + i\chi}{\sqrt{2}}$$

$$\begin{pmatrix} \phi \\ s \end{pmatrix} = \begin{pmatrix} \cos\theta & \sin\theta \\ -\sin\theta & \cos\theta \end{pmatrix} \begin{pmatrix} h_1 \\ h_2 \end{pmatrix}$$

- $\sin\theta \lesssim 0.3$ $\leftarrow$ Constrained by EWPT, h_2 direct search at LHC

PNGB DM model

C. Gross, O. Lebedev, TT, PRL (2017) [arXiv:1708.02253]

- χ is mass eigenstate itself $m_\chi^2 = \mu_S'^2$
  Invariant under $S \to S^\dagger$, $\Rightarrow \chi$ can be a DM candidate
- Higgs portal DM
- Scalar potential $\mathcal{V} = \mu_{h_1\chi\chi} h_1 \chi^2 + \mu_{h_2\chi\chi} h_2 \chi^2 + \cdots$

$$\mu_{h_1\chi\chi} = -\frac{m_{h_1}^2 \sin\theta}{v_s}, \quad \mu_{h_2\chi\chi} = \frac{m_{h_2}^2 \cos\theta}{v_s},$$

SM Yukawa int. $\mathcal{L} \supset y_q \Big(\cos\theta h_1 + \sin\theta h_2 \Big) \bar{q} q$

$$\lambda_H = \frac{\cos^2\theta m_{h_1}^2 + \sin^2\theta m_{h_2}^2}{v^2}, \quad \lambda_S = \frac{\sin^2\theta m_{h_1}^2 + \cos^2\theta m_{h_2}^2}{v_s^2},$$

$$\lambda_{HS} = \frac{\sin\theta\cos\theta(m_{h_2}^2 - m_{h_1}^2)}{v v_s}$$

UV completion

Y. Abe, TT, K. Tsumura, JHEP (2020) [arXiv:2001.03954]

- Origin of the soft breaking term? $\frac{m_\chi^2}{4}S^2 + \mathrm{H.c.}$

	Q_L	u_R^c	d_R^c	L	e_R^c	H	ν_R^c	S	Φ
$SU(3)_c$	$\mathbf{3}$	$\overline{\mathbf{3}}$	$\overline{\mathbf{3}}$	$\mathbf{1}$	$\mathbf{1}$	$\mathbf{1}$	$\mathbf{1}$	$\mathbf{1}$	$\mathbf{1}$
$SU(2)_L$	$\mathbf{2}$	$\mathbf{1}$	$\mathbf{1}$	$\mathbf{2}$	$\mathbf{1}$	$\mathbf{2}$	$\mathbf{1}$	$\mathbf{1}$	$\mathbf{1}$
$U(1)_Y$	$+1/6$	$-2/3$	$+1/3$	$-1/2$	$+1$	$+1/2$	0	0	0
$U(1)_{B-L}$	$+1/3$	$-1/3$	$-1/3$	-1	$+1$	0	$+1$	$+1$	$+2$

- Gauged $U(1)_{B-L}$ extension (New fields: ν_R, Φ)
- Potential $\mathcal{V} \supset \mu_c \Phi^* S^2 + \mathrm{h.c.} \to m_\chi^2 S^2$ at low energy
  The soft breaking term is induced.
- 3 ν_R for anomaly cancellation
- Seesaw for ν mass $\mathcal{L} \supset \Phi \nu_R \nu_R$

Direct detection (tree level)

C. Gross, O. Lebedev, TT, PRL (2017) [arXiv:1708.02253]

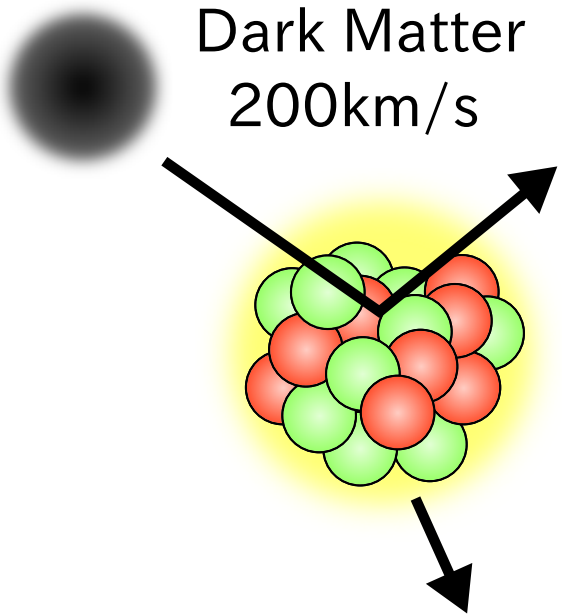

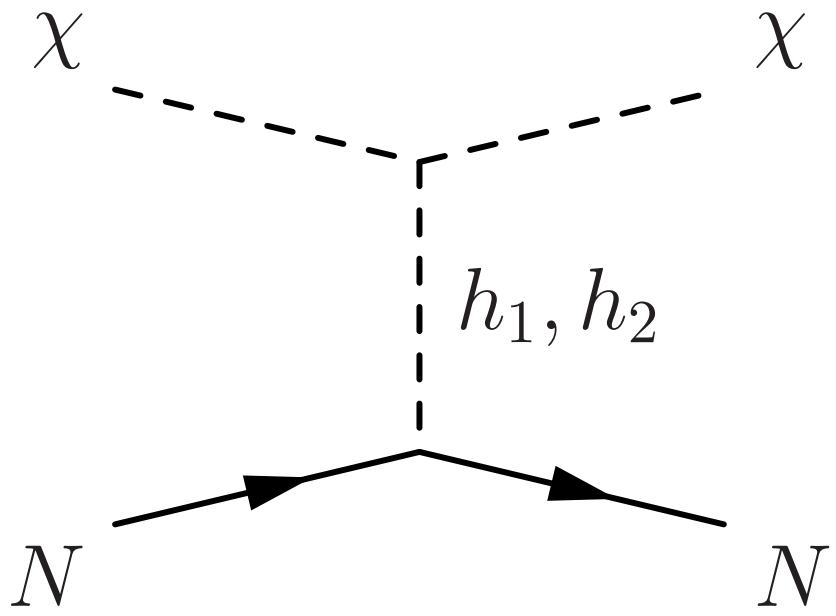

- Scattering amplitude cancels between h_1, h_2 mediated diagrams

$$i\mathcal{M} \sim i\left(\frac{m_{h_1}^2}{q^2 - m_{h_1}^2} - \frac{m_{h_2}^2}{q^2 - m_{h_2}^2}\right) \sim i\frac{q^2(m_{h_1}^2 - m_{h_2}^2)}{m_{h_1}^2 m_{h_2}^2} \quad \to \quad 0$$

Direct detection (tree level)

C. Gross, O. Lebedev, TT, PRL (2017) [arXiv:1708.02253]

Rewrite with $S = \frac{(v_s + s)}{\sqrt{2}} e^{i\chi/v_s} \quad \Rightarrow \quad \mathcal{L} \supset \frac{1}{v_s} s \left[(\partial_\mu \chi)^2 - m_\chi^2 \chi^2 \right]$

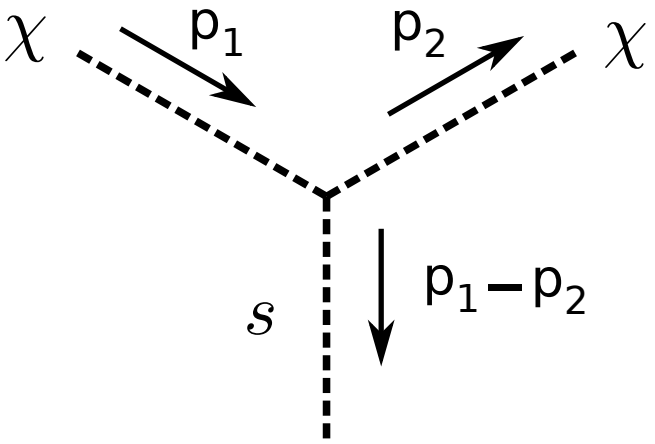

$$\to i\mathcal{M} \sim -\frac{i}{v_s}(p_1 - p_2)^2 \sim -\frac{i}{v_s} m_\chi^2 v_\chi^2 \to 0$$

$$v_\chi \sim \mathcal{O}(10^{-3})$$

- Cancellation is due to nature of Goldstone boson
- All interactions are written with derivative couplings $\mathcal{L}_{\rm int} = \mathcal{L}_{\rm int}(\partial_\mu \chi)$

Direct detection (1-loop level)

D. Azevedo et al., JHEP [arXiv:1810.06105]
K. Ishiwata, TT, JHEP [arXiv:1810.08139]
S. Glaus et al., JHEP [arXiv:2008.12985]

- Compute Feynman diagrams at 1-loop level

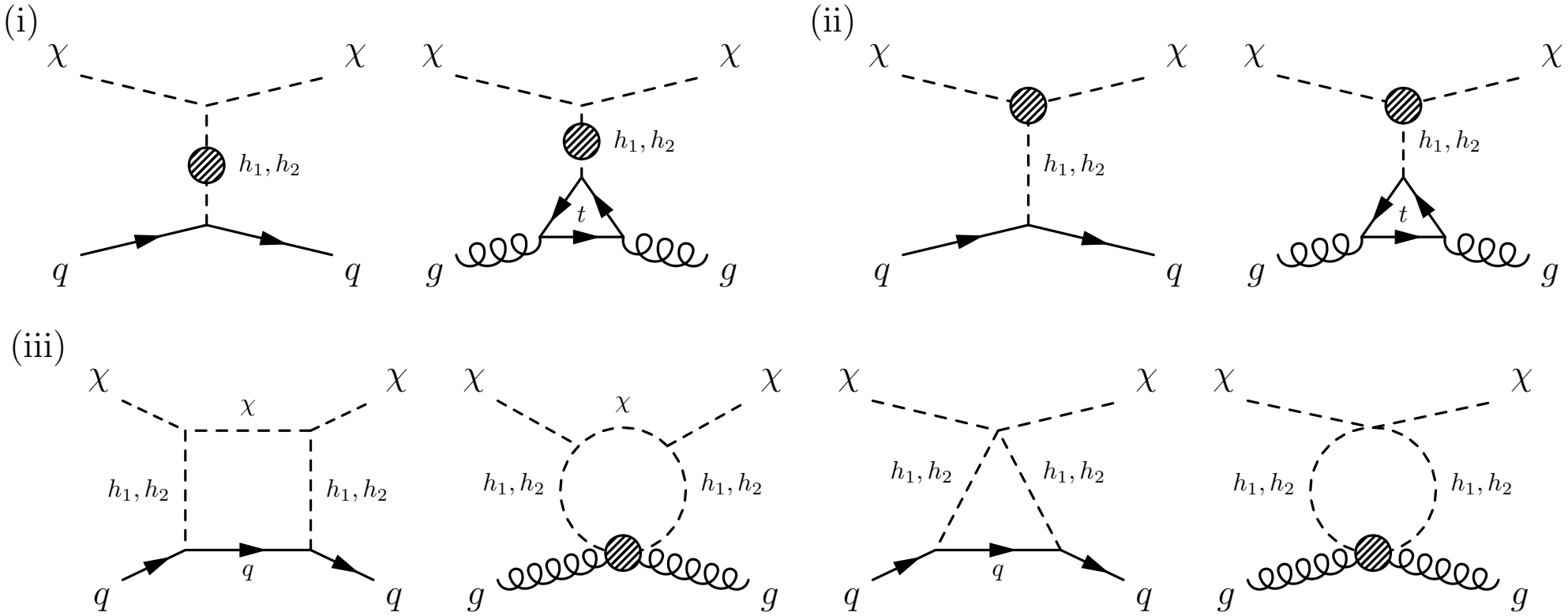

- (i) self-energy correction
- (ii) vertex correction
- (iii) box and triangle $\rightarrow$ two Yukawa couplings
  $\rightarrow$ sub-dominant in most cases

Numerical analysis (1-loop level)

K. Ishiwata, TT, JHEP [arXiv:1810.08139]

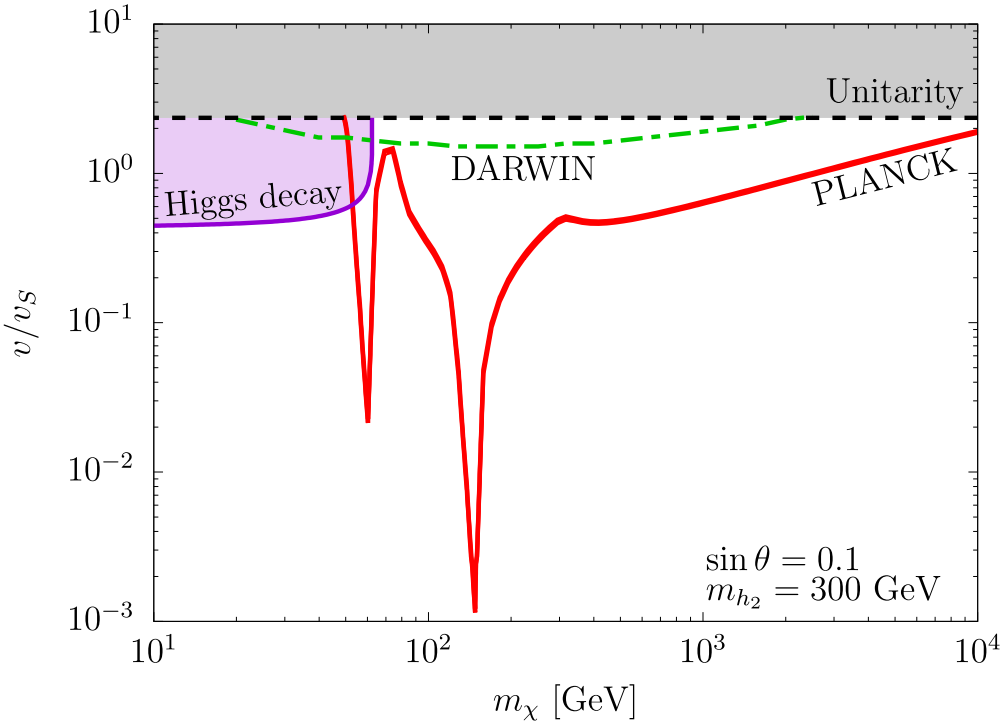

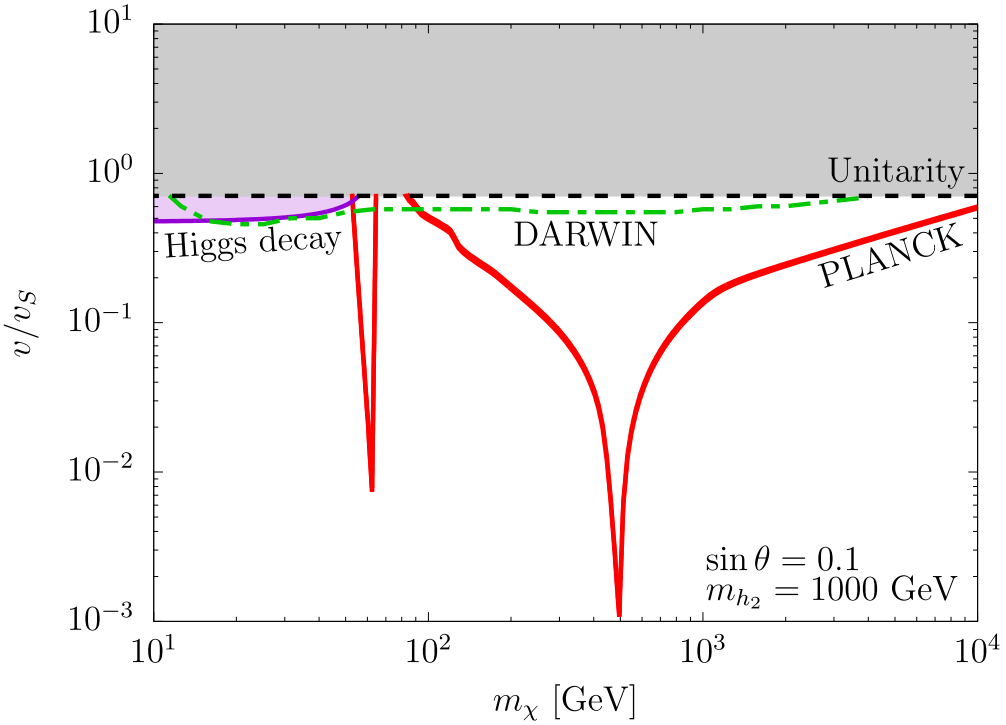

- Only 4 independent parameters ($m_\chi,\ m_{h_2},\ \sin\theta,\ v_s\ (\lambda_S)$)
- $\sin\theta = 0.1$
- Invisible Higgs decay $\mathrm{Br}(h_1 \to \mathrm{inv}) \lesssim 20\%$ at LHC
- $\sigma^p_{\mathrm{SI}} = \mathcal{O}(10^{-48})\ \mathrm{cm}^2$ at most
- Unitarity bound: $\lambda_S \leq 8\pi/3$

Numerical analysis (1-loop level)

K. Ishiwata, TT, JHEP [arXiv:1810.08139]

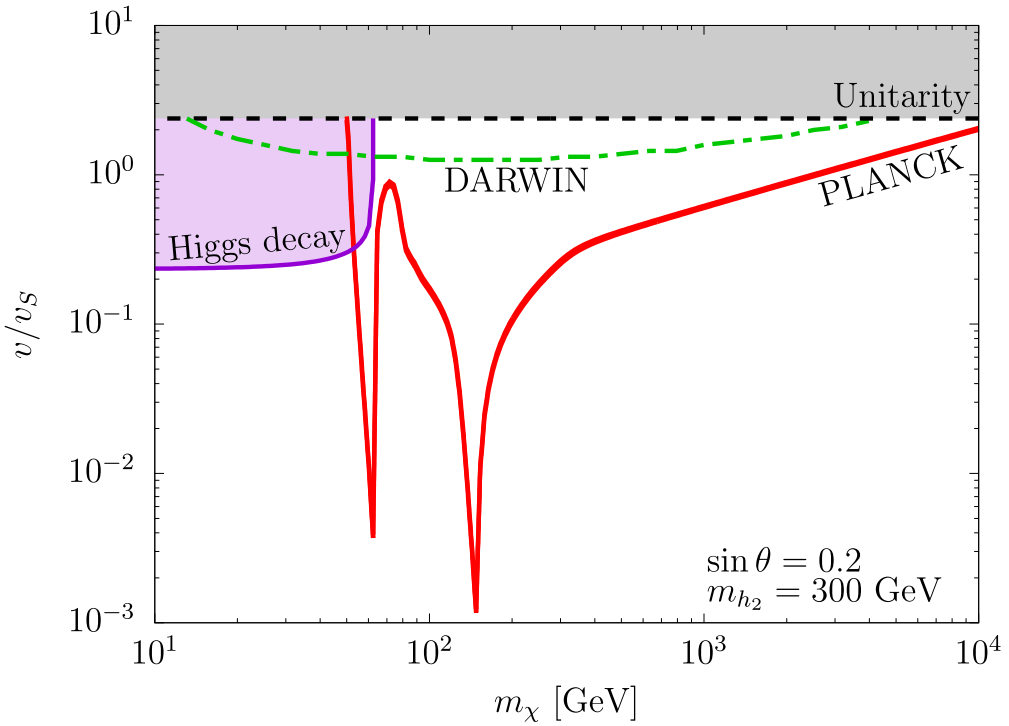

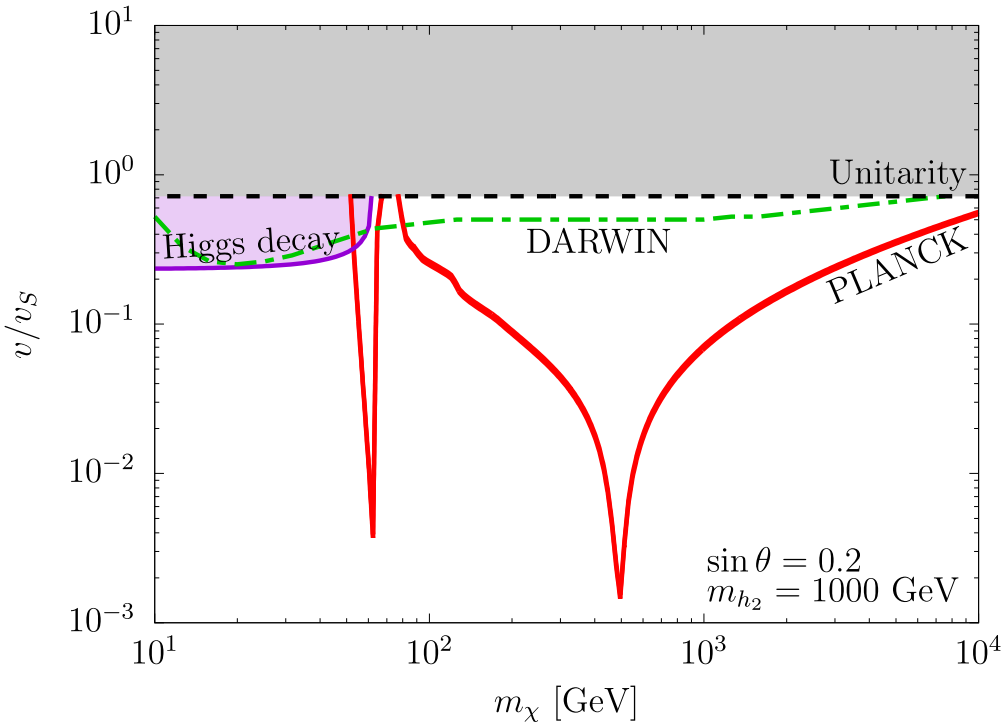

- $\sin\theta = 0.2$
- Invisible Higgs decay $\mathrm{Br}(h_1 \to \mathrm{inv}) \lesssim 20\%$ at LHC
- $\sigma^p_{\mathrm{SI}} = \mathcal{O}(10^{-48})\ \mathrm{cm}^2$ at most
- Unitarity bound: $\lambda_S \leq 8\pi/3$

Pseudo-Nambu-Goldstone DM with light mediator h_2

Light mediator h_2

Abe, TT, PLB (2021) [arXiv:2108.10647]

- $m_{h_2} \ll m_\chi$ $\quad (m_{h_2} \gg m_\chi$ since $\mathbb{Z}_2 \to U(1)$?)

  UV completion $\mathcal{V} \supset \mu \Phi^* S^2 \to \mu \langle \Phi \rangle S^2 \;\Rightarrow\; m_{h_2} \ll m_\chi$ if $\langle S \rangle \ll \langle \Phi \rangle$

- Main annihilation channel: $\chi\chi \to h_2 h_2$

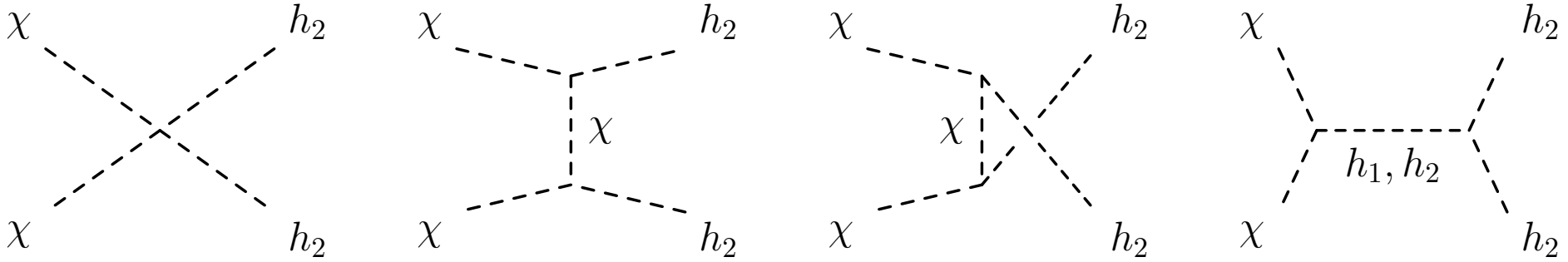

$$\sigma_{h_2 h_2} v_{\rm rel} = \frac{\lambda_S^2}{16\pi s} \left| 1 + \frac{m_{h_1}^2}{m_{h_2}^2} \frac{\sin^2\theta s}{s - m_{h_1}^2 + i m_{h_1} \Gamma_{h_1}} \right|^2$$

- The other channels: $\chi\chi \to WW, ZZ, f\overline{f}, h_1 h_1, h_1 h_2$

  $\sigma v_{\rm rel} \propto \sin^2\theta$

- We focus on the mass range $20\ \mathrm{MeV} \lesssim m_{h_2} \lesssim 200\ \mathrm{MeV}$

Event rate

Abe, TT, PLB (2021) [arXiv:2108.10647]

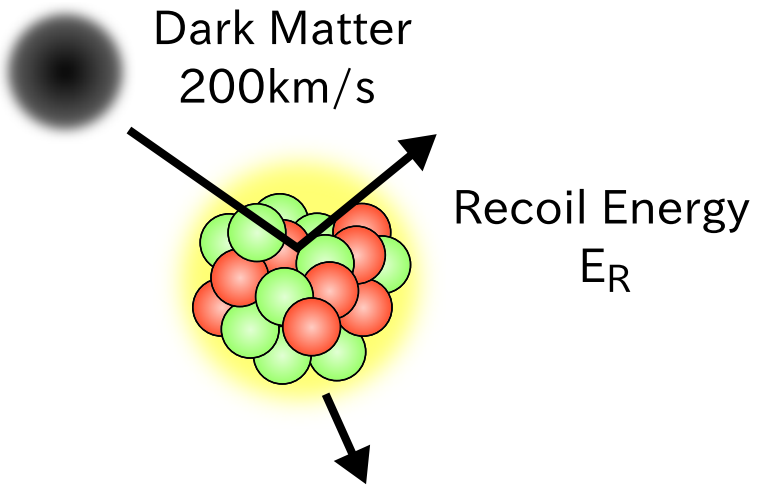

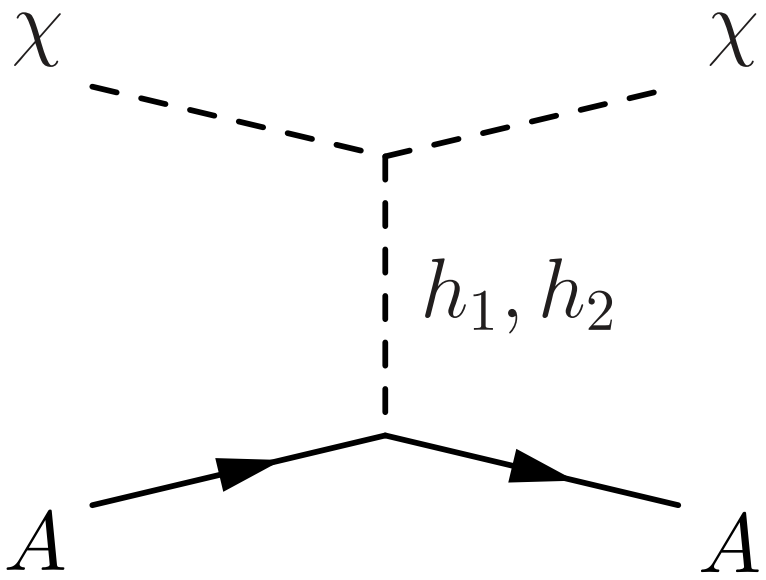

- Differential cross section

$$\frac{d\sigma_A}{dE_R} \approx \frac{m_A \kappa_A^2}{8\pi m_\chi^2 v_\chi^2} \frac{\sin^2\theta}{v^2 v_s^2} \frac{q^4}{(q^2 - m_{h_2}^2)^2} F^2(E_R) \quad \overset{v_\chi \to 0}{\longrightarrow} \quad 0$$

$$= \frac{m_A \kappa_A^2}{8\pi m_\chi^2 v_\chi^2} \frac{\sin^2\theta}{v^2 v_s^2} F^2(E_R) \begin{cases} 1 & \text{for} \quad q^2 \gg m_{h_2}^2 \\ \frac{q^4}{m_{h_2}^4} & \text{for} \quad q^2 \ll m_{h_2}^2 \end{cases}$$

- PNGB DM can be tested by DD if the mediator is light enough.

Energy spectrum

Abe, TT, PLB (2021) [arXiv:2108.10647]

Hambye et al., PRD (2018) [arXiv:1807.05022]

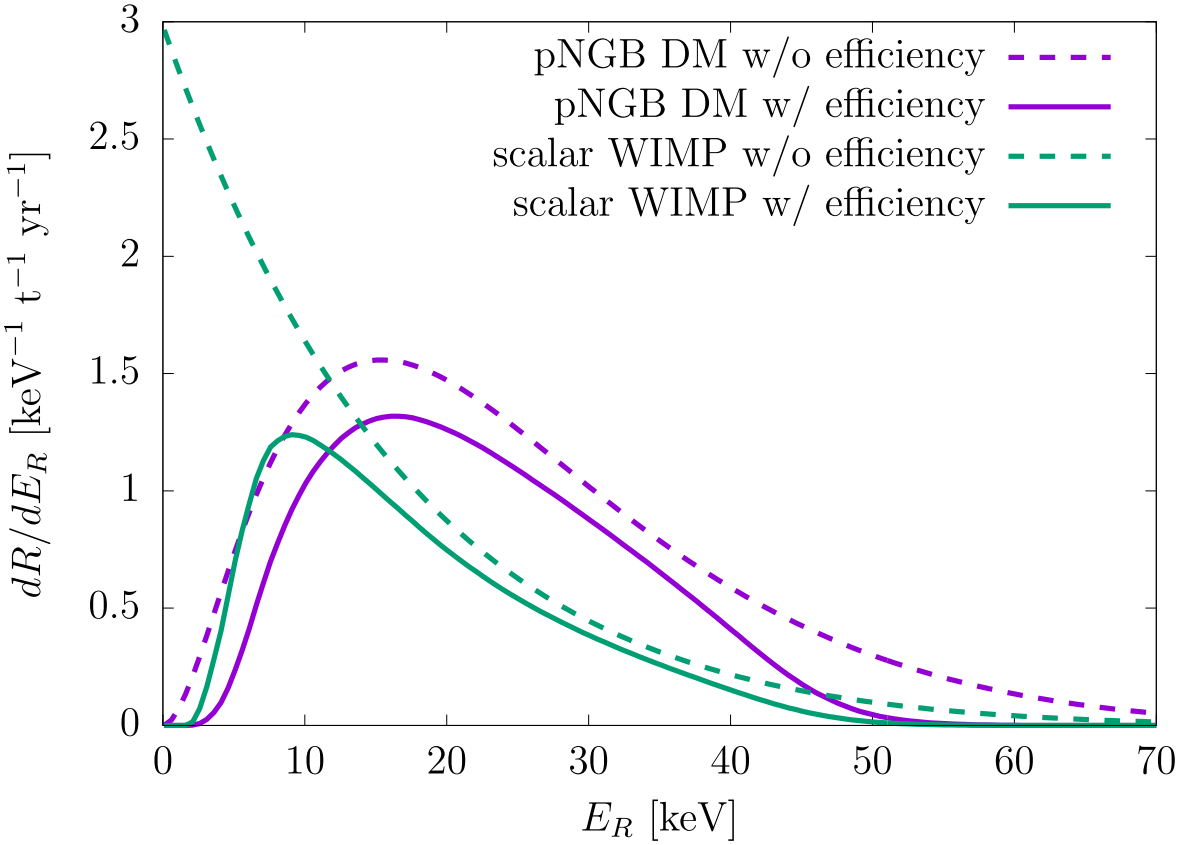

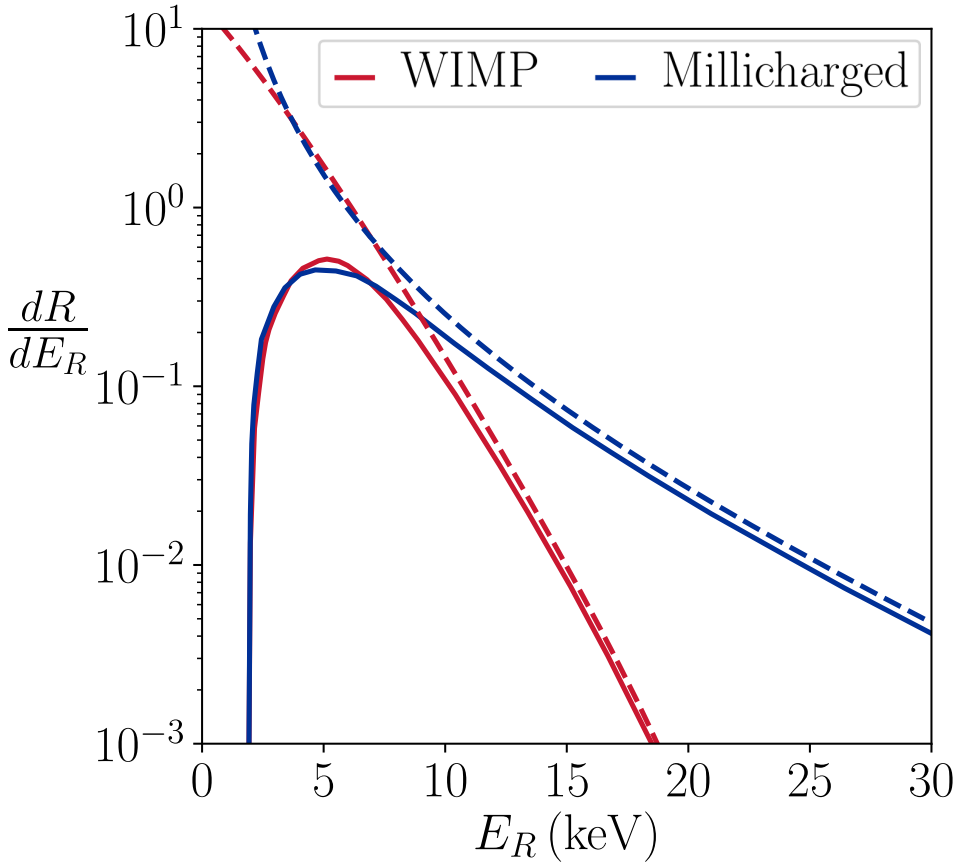

- Energy spectrum for pNGB DM is different from normal WIMP.
- But similar energy spectra can be induced from inelastic scattering and the other momentum dependent scatterings.

Numerical results ($\sin\theta = 3 \times 10^{-5}$)

Abe, TT, PLB (2021) [arXiv:2108.10647]

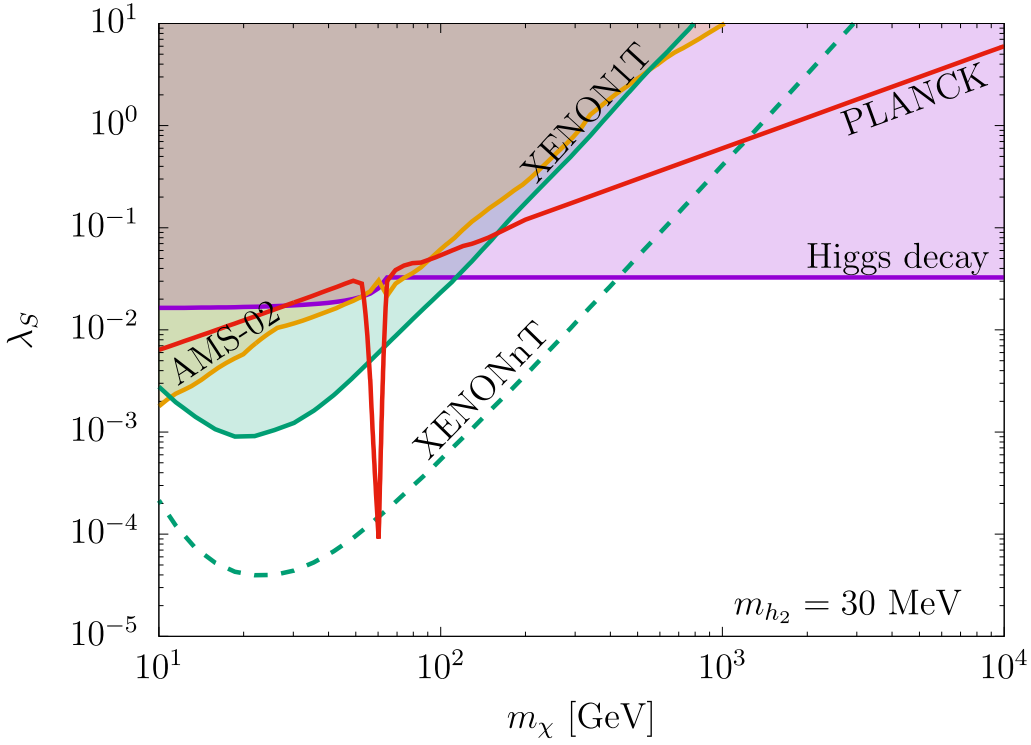

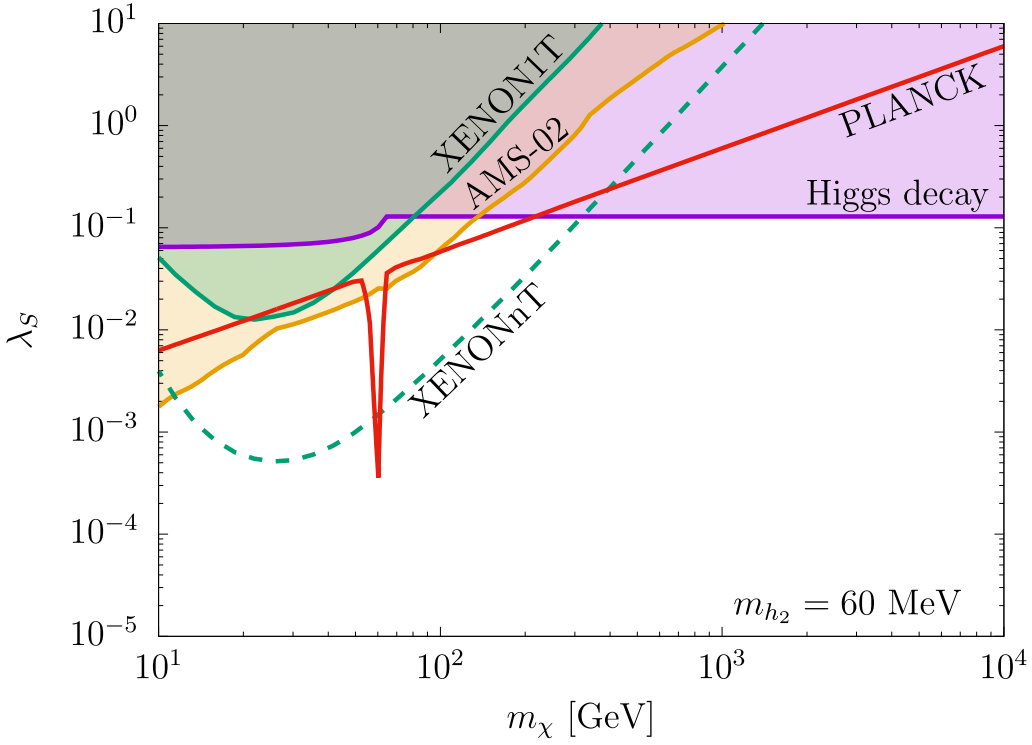

- Higgs resonance at $m_\chi \approx m_{h_1}/2$
- Right plot: $100\ \mathrm{GeV} \lesssim m_\chi \lesssim 200\ \mathrm{GeV}$ can be tested by XENONnT.

Numerical results ($\sin\theta = 3 \times 10^{-5}$)

Abe, TT, PLB (2021) [arXiv:2108.10647]

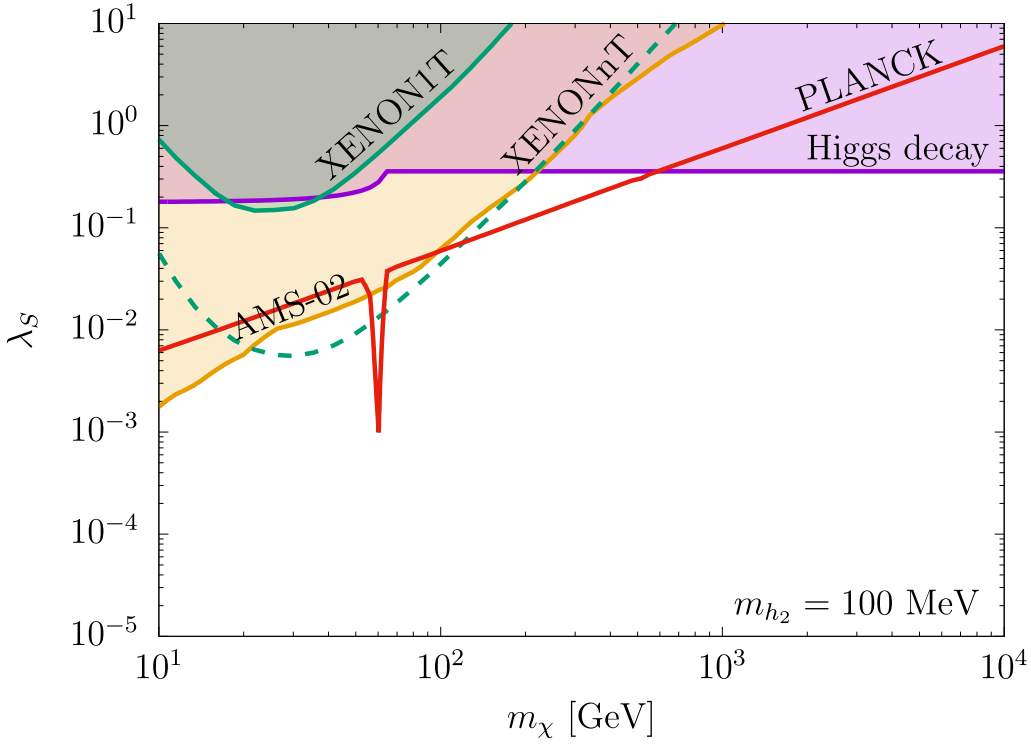

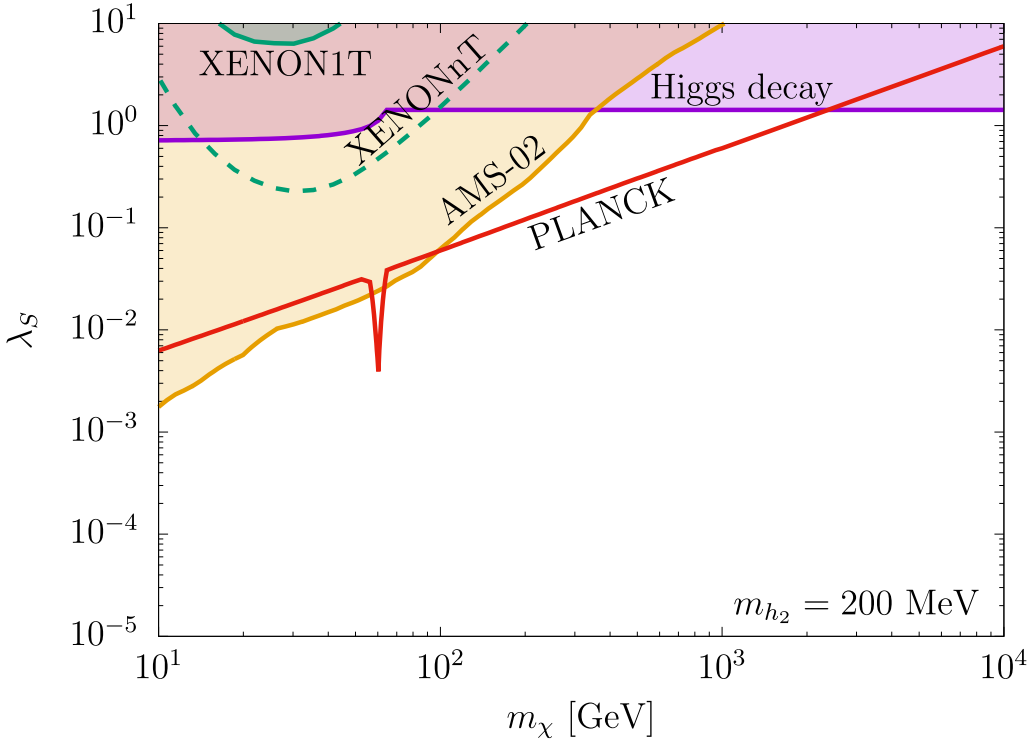

- Larger m_{h_2} case
- More parameter space is allowed.
- No sensitivity for direct detection.

Summary

1. Thermal WIMP DM is strongly constrained by recent direct detection experiments.
   $\Rightarrow$ PNGB DM can naturally avoid it.
2. For $m_{h_2} \gtrsim m_\chi$, elastic cross section with nucleon (1-loop) is $\sigma^N_{\rm SI} = \mathcal{O}(10^{-48})\ {\rm cm}^2$ at most.
3. For light mediator h_2 ($m_{h_2} \lesssim 200\ {\rm MeV}$),
   non-zero direct detection rate emerges.
   · Some region can be tested by XENONnT.
   · Energy spectrum can differ from normal WIMP.

Back Up

Domain wall problem

- Domain walls due to spontaneous breaking of $\mathbb{Z}_2$ symmetry
  $\Rightarrow$ distort CMB
- Solutions: · UV compeltion
  · low energy inflation after the $\mathbb{Z}_2$ breaking
  · decay before BBN (making the domain wall unstable)

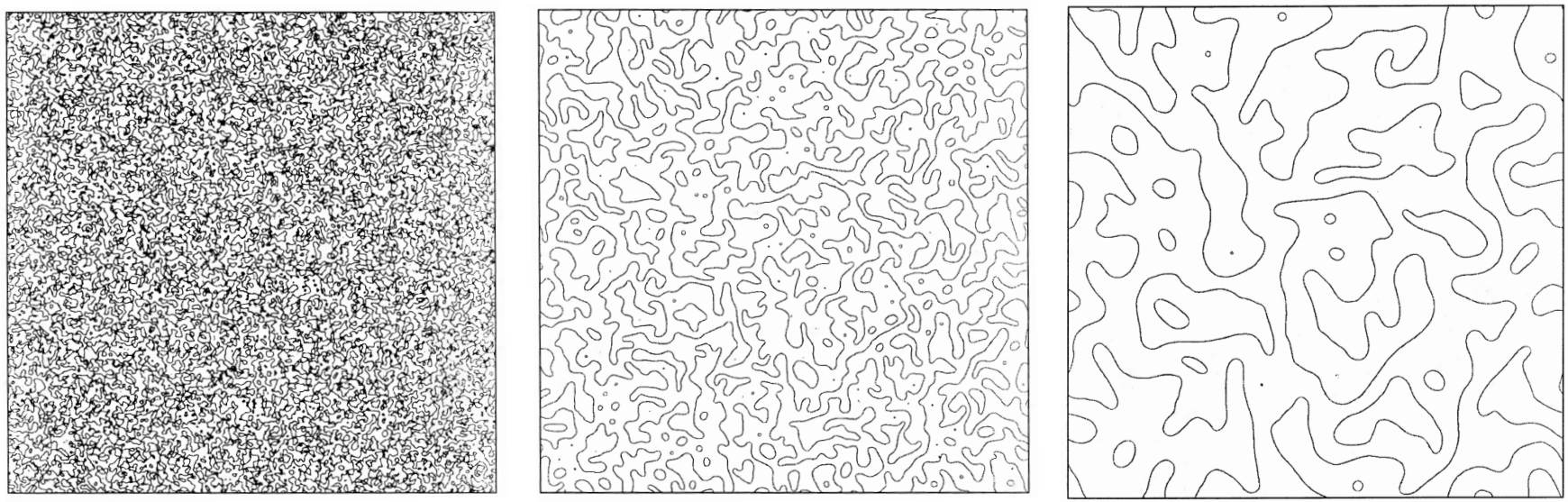

Press, Ryden, Spergel ApJ (1989)

WIMP search status

Indirect detection (Gamma-rays from dSphs)

$\chi\chi \to b\bar{b}$

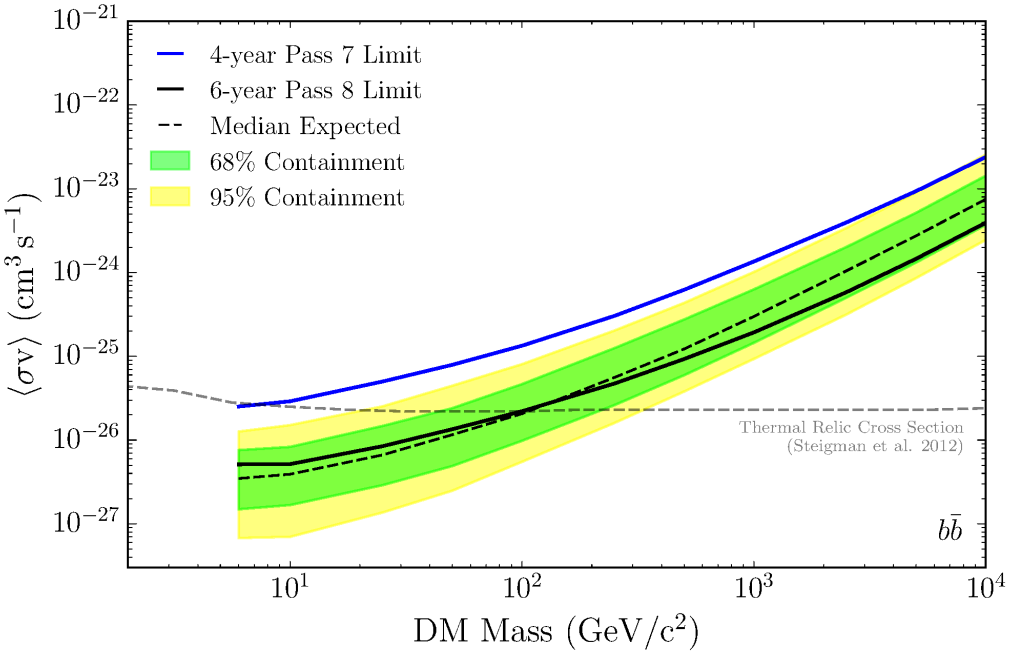

$\chi\chi \to \tau^+\tau^-$

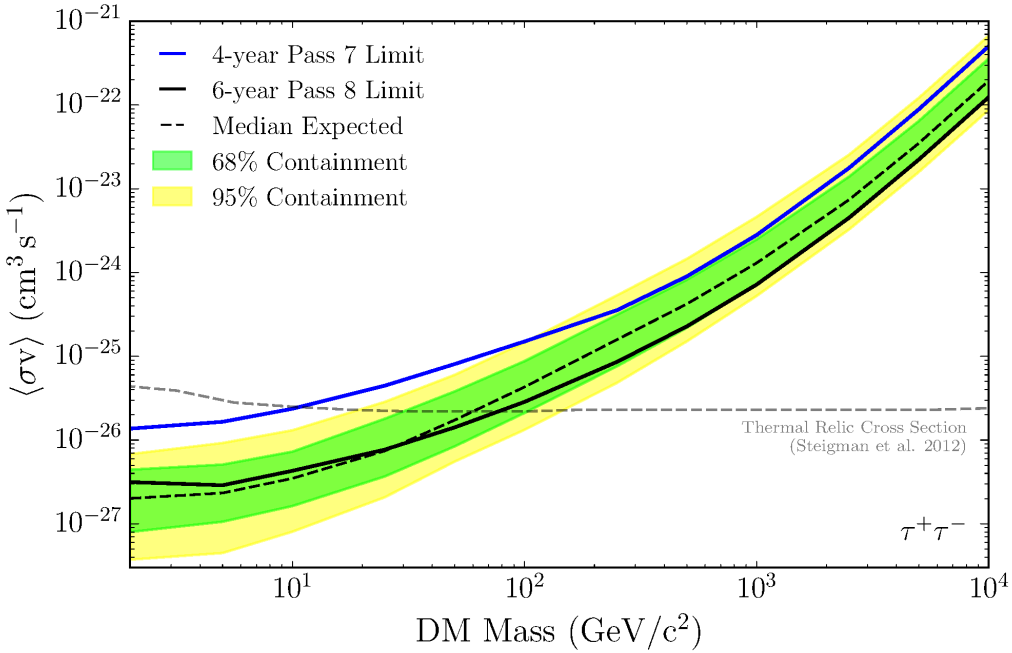

Fermi-LAT, PRL (2015) arxiv:1503.02641

- A lot of gamma-rays are generated if final state particles are charged.
- $m_{\rm DM} \lesssim 100$ GeV is excluded if thermal WIMP scenarios are assumed.
- $\langle\sigma v\rangle \sim 10^{-26}\ {\rm cm}^3/{\rm s}$ for thermal DM

Bound on $\sin\theta$

A. Falkowski et al., JHEP 1505 (2015) [arxiv:1502.01361]

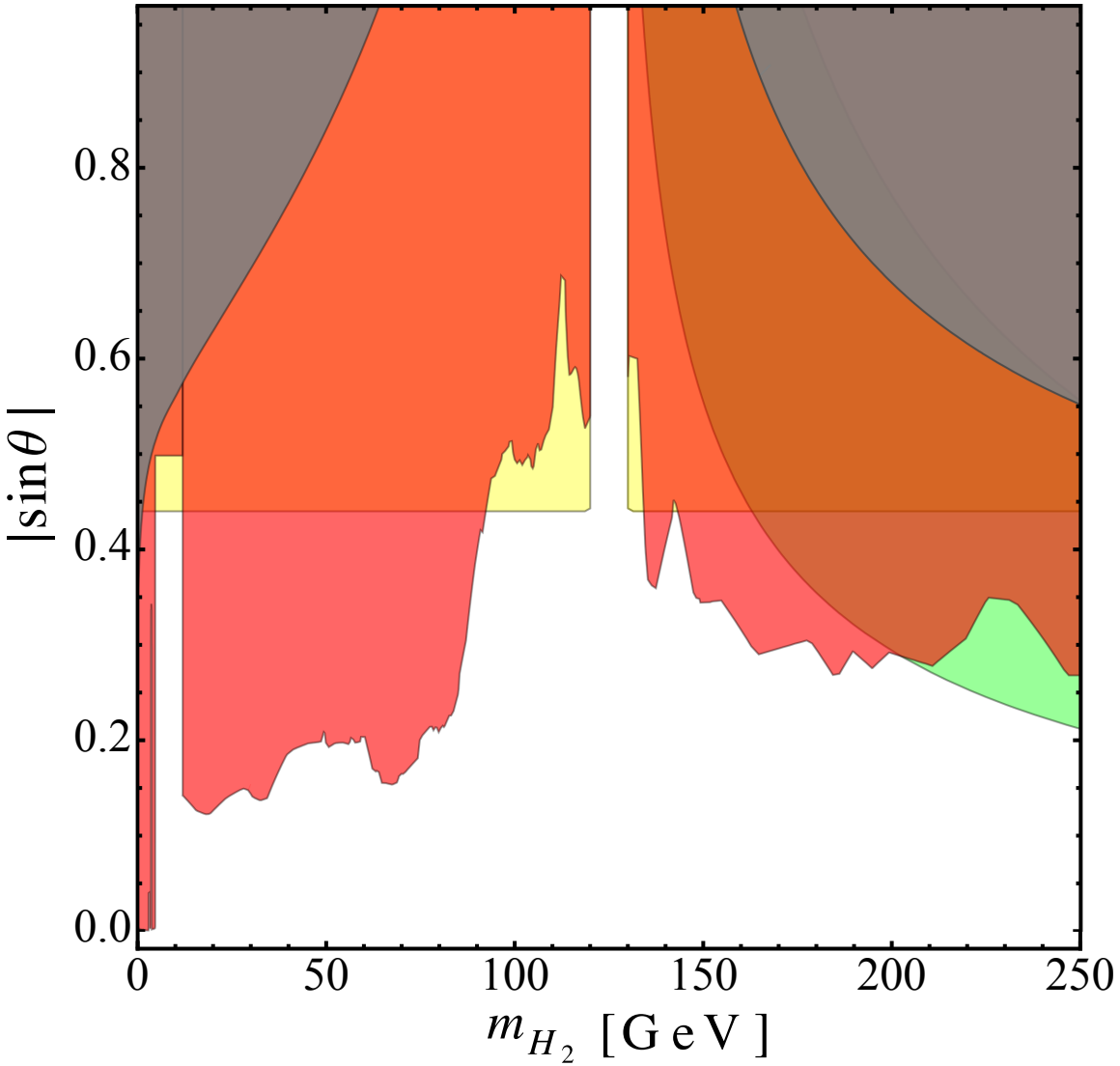

- Red: h_2 direct search at LHC
- Yellow: h_1 coupling measurements
- Green: Favored region from stability of scalar potential
- Gray: Electroweak precision tests
- $|\sin\theta| \lesssim 0.3$ if $m_{h_2} \gtrsim m_{h_1}$
- $m_\chi \lesssim m_{h_2}$ (above EW scale)

The pNGB DM model

C. Gross, O. Lebedev, TT, PRL (2017) [arXiv:1708.02253]

- Cubic couplings

$$\mathcal{V} \supset \frac{\kappa_{111}}{3!}h_1^3 + \frac{\kappa_{112}}{2!}h_1^2 h_2 + \frac{\kappa_{122}}{2!}h_1 h_2^2 + \frac{\kappa_{222}}{3!}h_2^3$$

$$\kappa_{111} = 3m_{h_1}^2 \left(-\frac{\sin^3\theta}{v_s} + \frac{\cos^3\theta}{v}\right),$$

$$\kappa_{112} = \left(2m_{h_1}^2 + m_{h_2}^2\right)\sin\theta\cos\theta\left(\frac{\sin\theta}{v_s} + \frac{\cos\theta}{v}\right),$$

$$\kappa_{122} = \left(m_{h_1}^2 + 2m_{h_2}^2\right)\sin\theta\cos\theta\left(-\frac{\cos\theta}{v_s} + \frac{\sin\theta}{v}\right),$$

$$\kappa_{222} = 3m_{h_2}^2 \left(\frac{\cos^3\theta}{v_s} + \frac{\sin^3\theta}{v}\right),$$

Event rate

Abe, TT, PLB (2021) [arXiv:2108.10647]

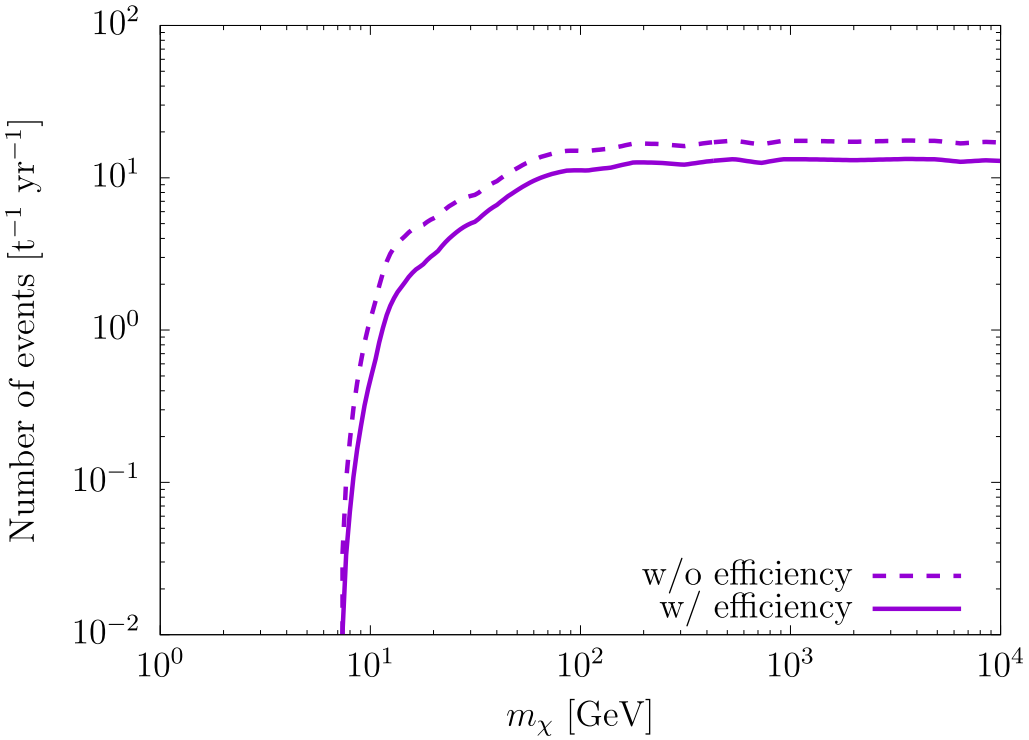

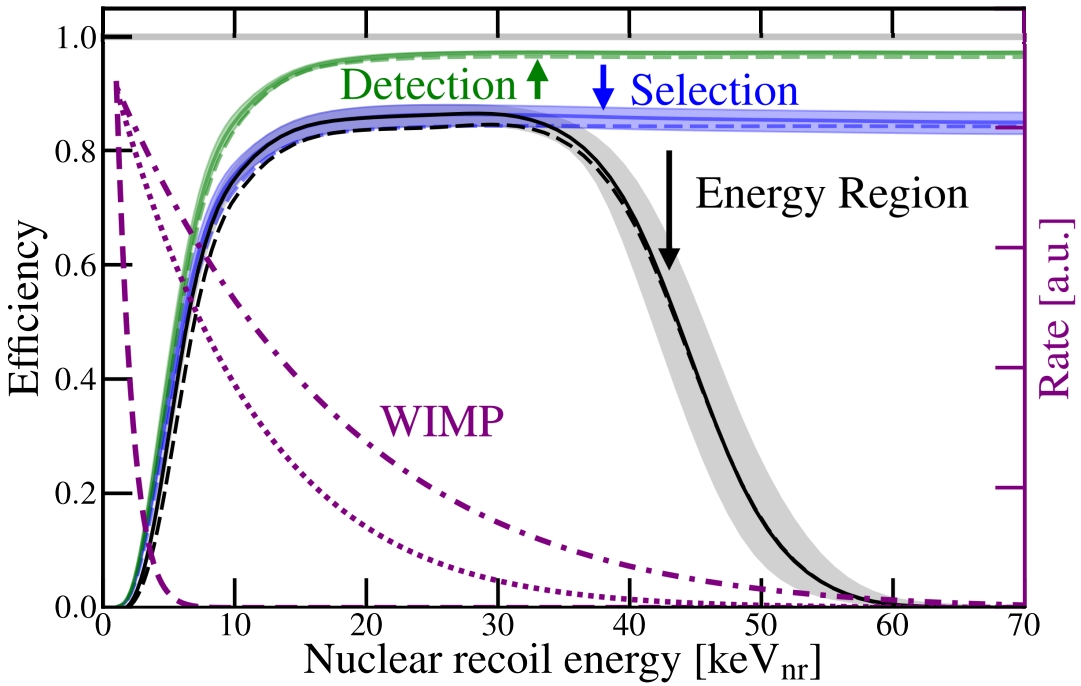

XENON1T, PRL (2018) [arXiv:1805.12562]

- Event rate

$$\frac{dR}{dE_R} = \frac{\rho_\odot}{m_\chi} N_T \int_{v>v_{\min}} \frac{d\sigma_A}{dE_R} v_\chi f_\odot(\boldsymbol{v}_\chi) d^3 v_\chi$$

- Total event rate R can be compared with experiments.

Numerical results ($\sin\theta = 10^{-4}$)

Abe, TT, PLB (2021) [arXiv:2108.10647]

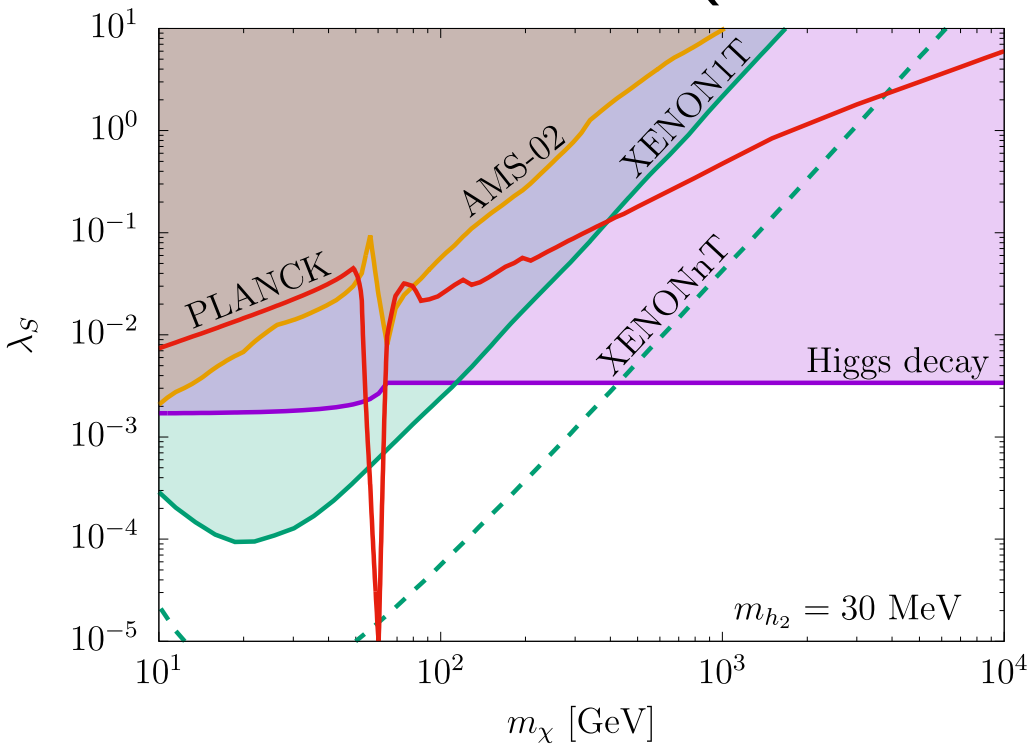

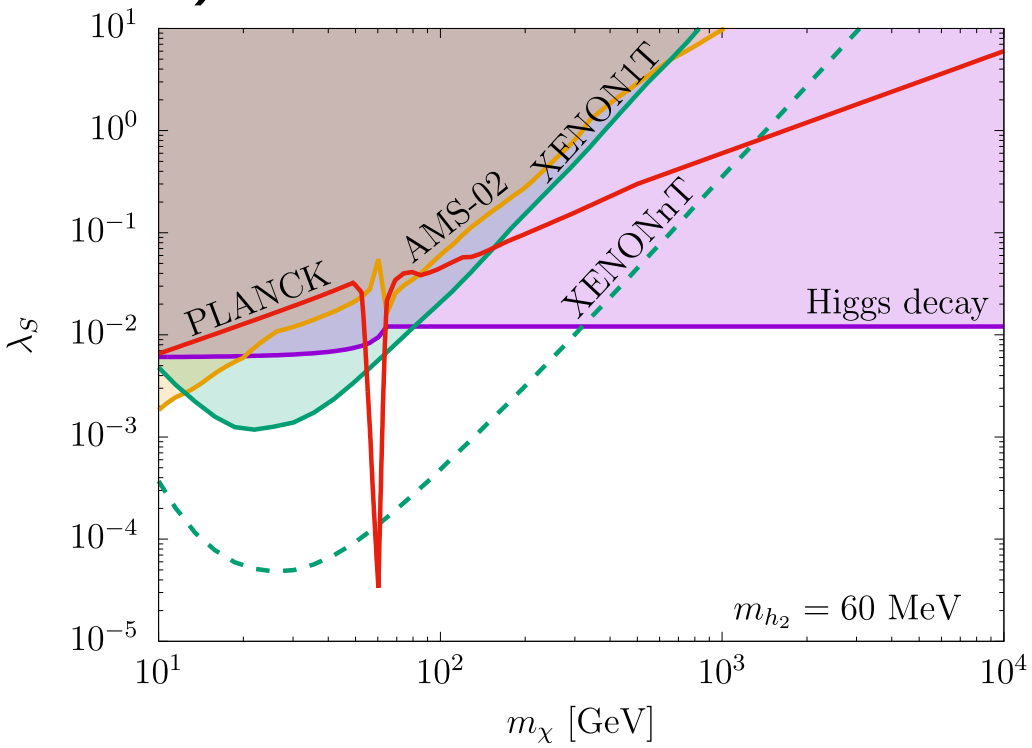

- Resonance at $2m_\chi \sim m_{h_1}$
- Only resonance region can be allowed.

Numerical results ($\sin\theta = 10^{-4}$)

Abe, TT, PLB (2021) [arXiv:2108.10647]

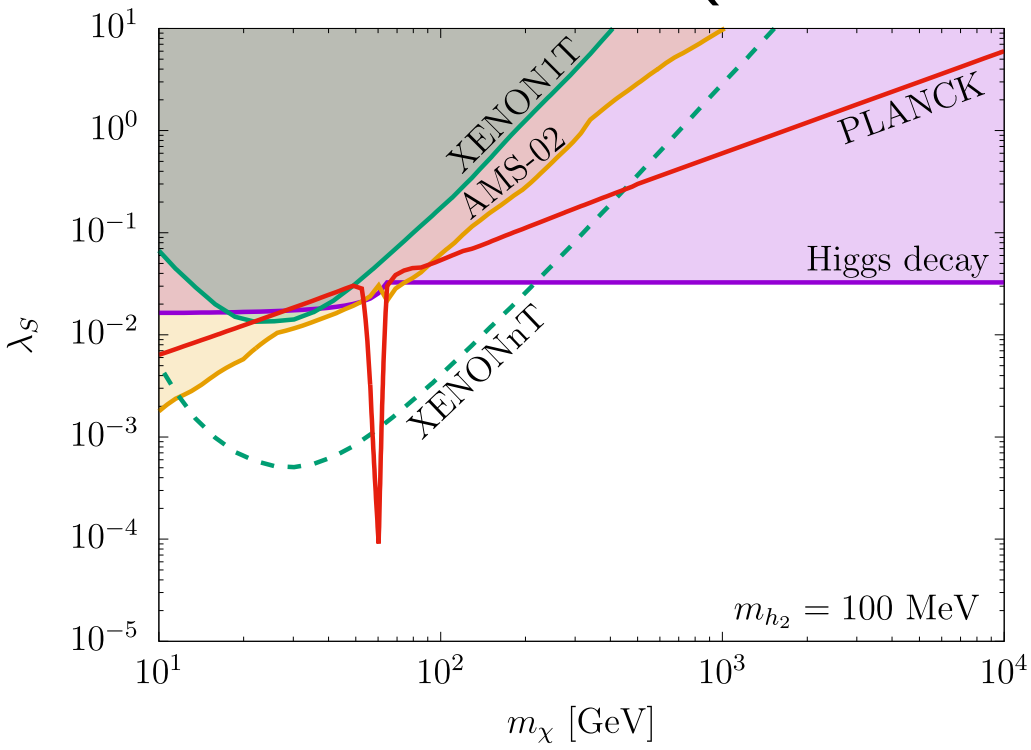

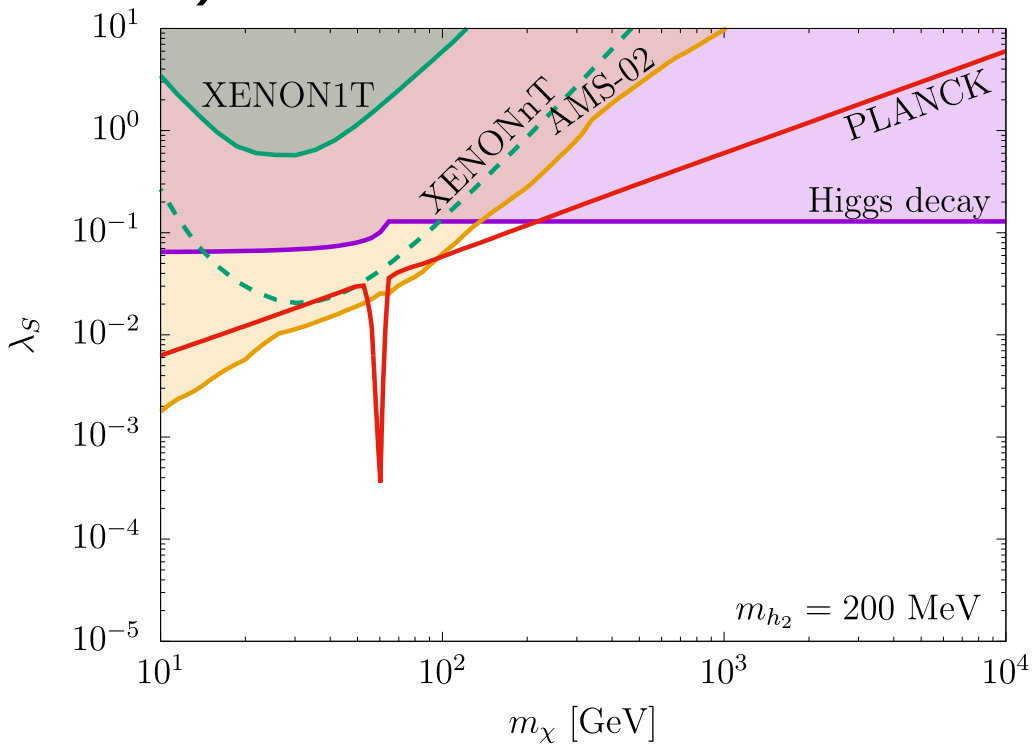

- The other parameter region is allowed for heavier m_{h_2}.
- But direct detection rate becomes small as expected.

Mixing angle

Winkler, PRD (2019) [arXiv:1809.01876]

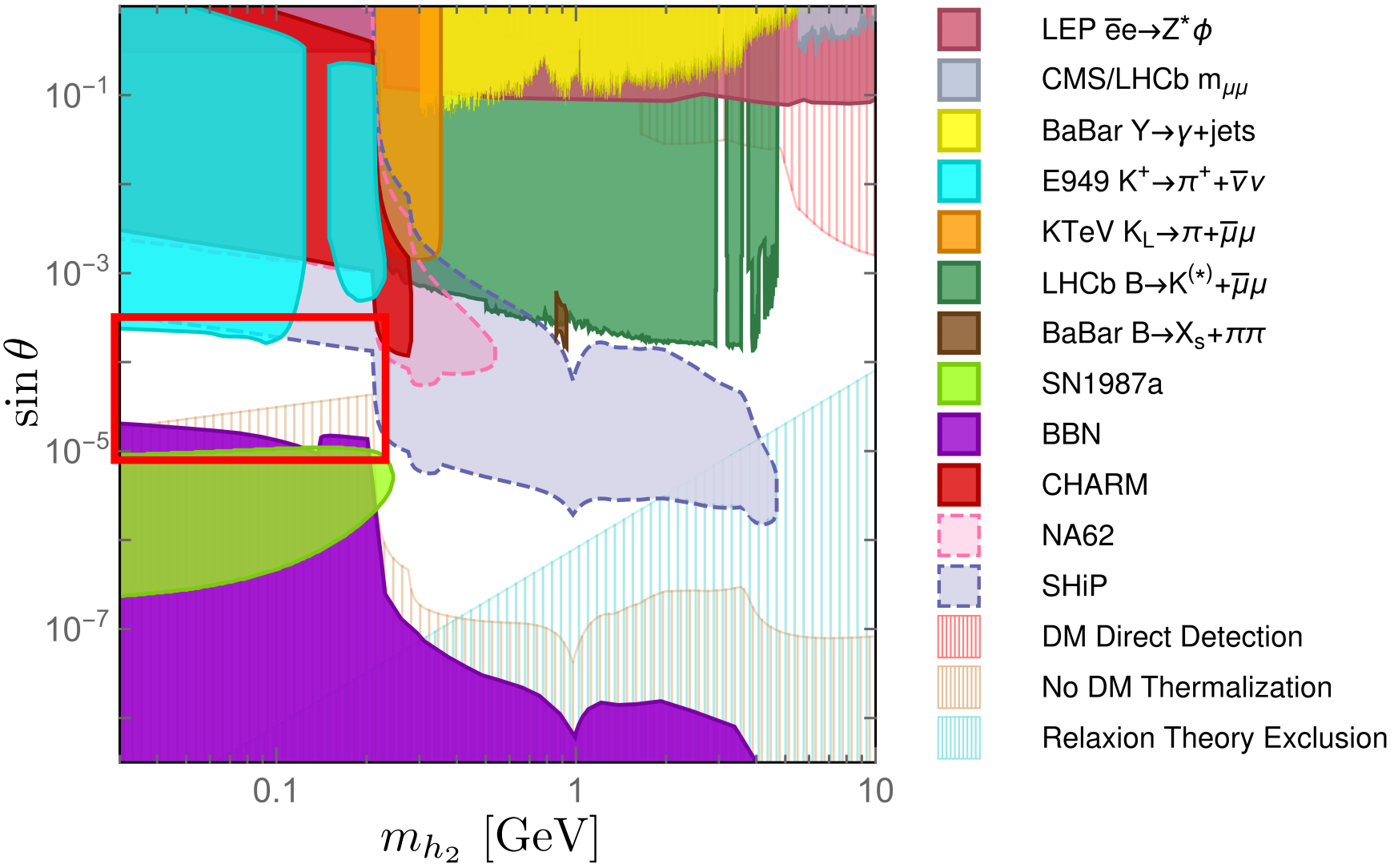

- $2 \times 10^{-5} \lesssim \sin\theta \lesssim 10^{-4}$

Limit on $\sigma_{h_2 h_2} v_{\rm rel}$

Abe, TT, PLB (2021) [arXiv:2108.10647]

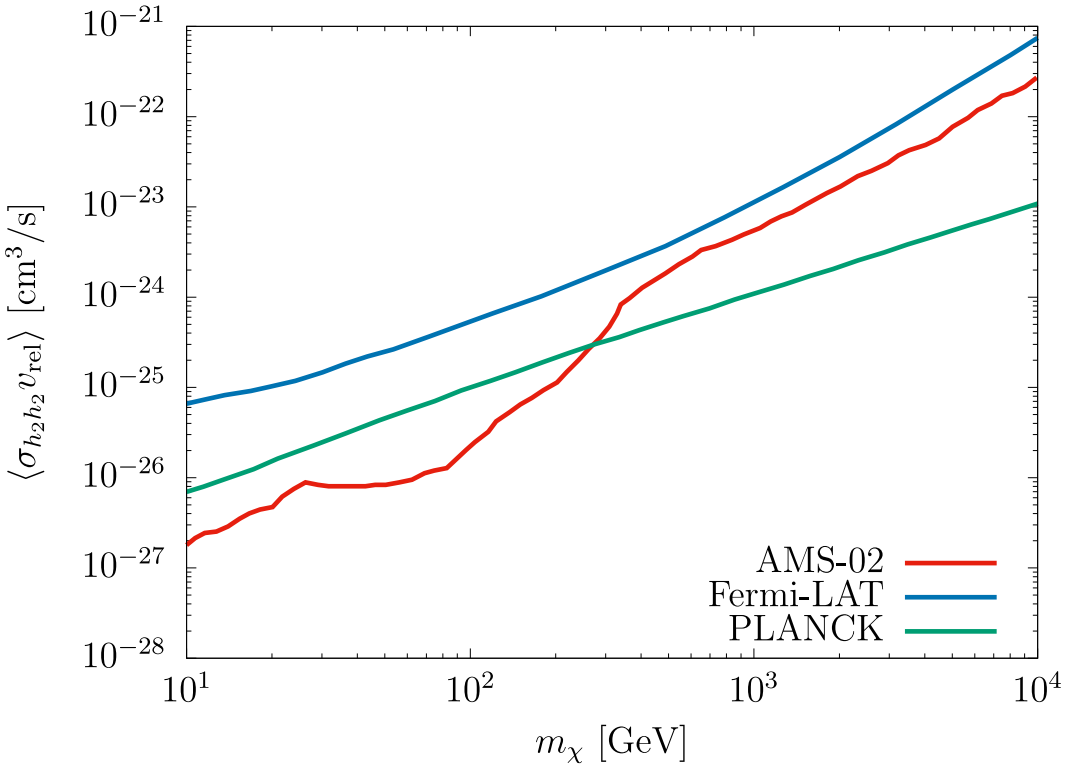

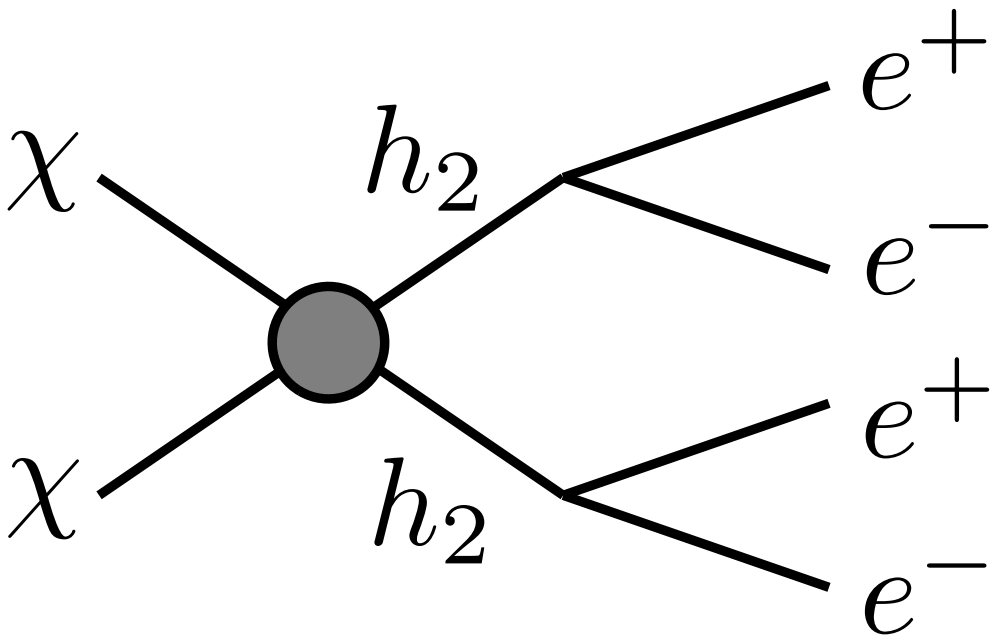

Elor et al., JCAP (2016) [arXiv:1511.08787]

- $\chi\chi \to e^+e^-e^+e^-$ (AMS-02), gamma-rays (Fermi-LAT) and CMB (PLANCK)
- Model-independent indirect detection constraints from cascade decays

Higgs decays

Abe, TT, PLB (2021) [arXiv:2108.10647]

- $h_1 \to h_2 h_2, \chi\chi$ contributes to Higgs invisible decay.

$$\Gamma_{h_2 h_2} = \frac{\kappa_{122}^2}{32\pi m_{h_1}} \sqrt{1 - 4\frac{m_{h_2}^2}{m_{h_1}^2}} \approx \frac{\lambda_S m_{h_1}^3 \sin^2\theta}{32\pi m_{h_2}^2},$$

$$\Gamma_{\chi\chi} \approx \frac{\lambda_S m_{h_1}^3 \sin^2\theta}{32\pi m_{h_2}^2} \sqrt{1 - 4\frac{m_\chi^2}{m_{h_1}^2}}$$

- Experimental limit: $\mathrm{Br}_{\mathrm{inv}} \leq 0.11$
  Higgs signal strength is translated into the constraint of branching ratio

  $\Rightarrow \lambda_S \gtrsim \mathcal{O}(1)$ region is excluded.

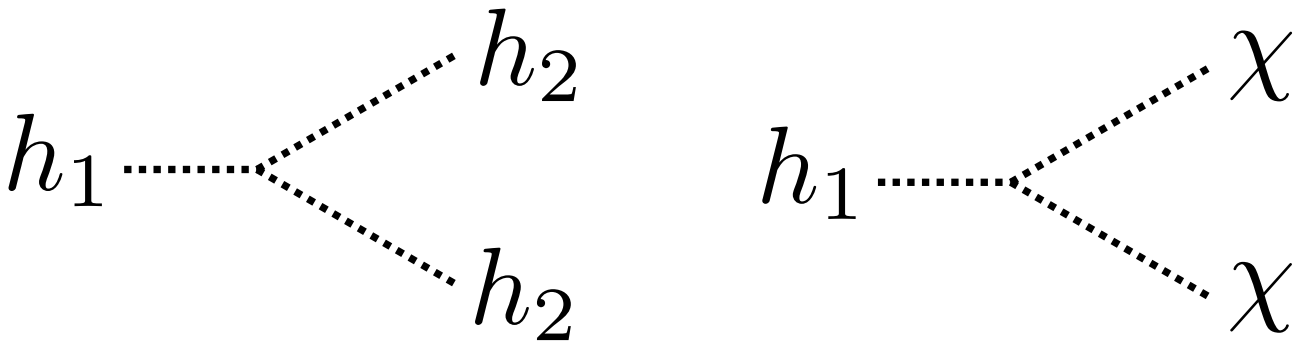

Energy spectrum 2

McCabe, PRD (2010) [arXiv:1005.0579]

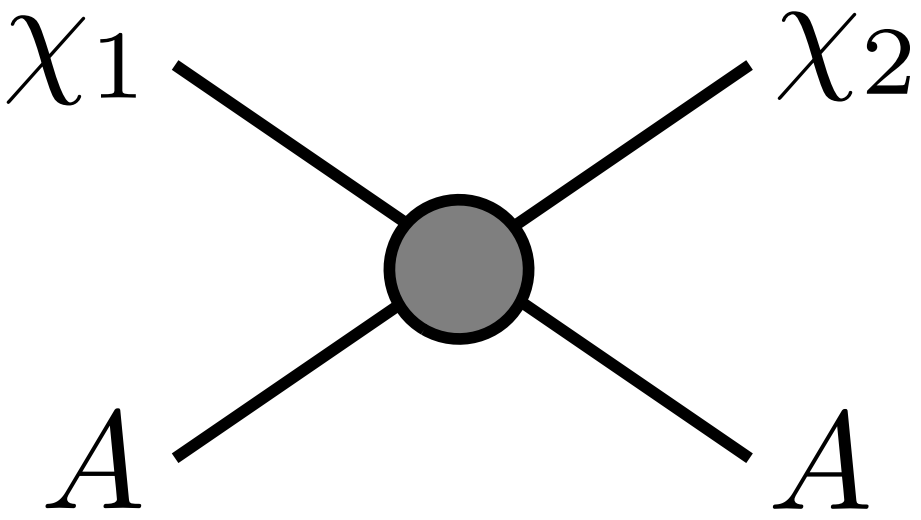

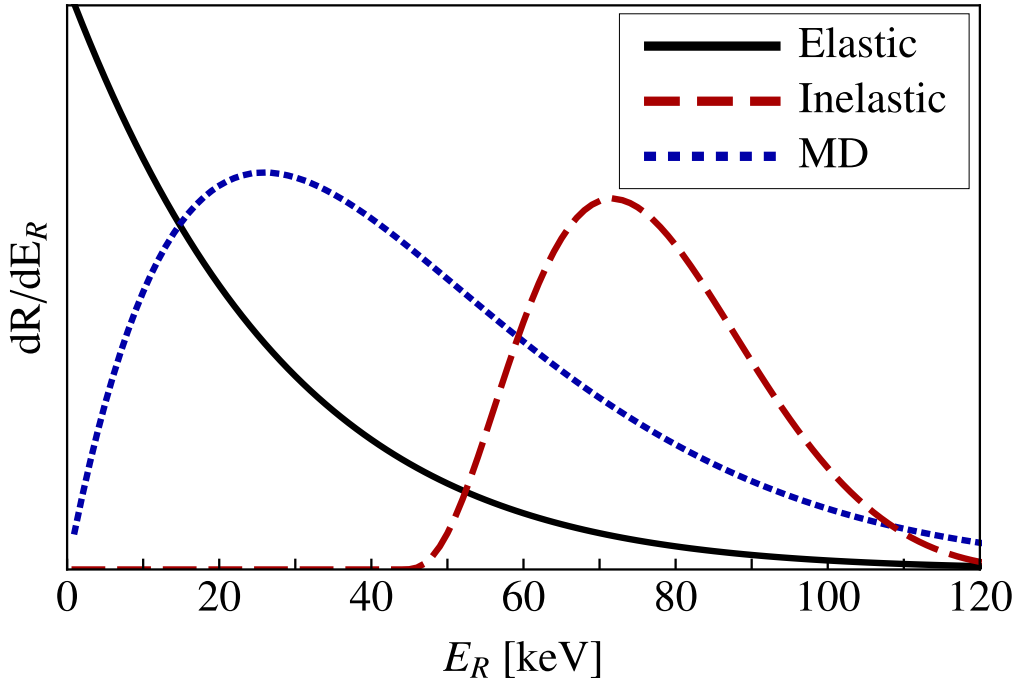

- Inelastic scattering $\chi_1 A \to \chi_2 A$ where $m_{\chi_1} < m_{\chi_2}$ and $\delta = m_{\chi_2} - m_{\chi_1}$
- $v_{\rm min} = \sqrt{\dfrac{1}{2 m_A E_R}} \left(\dfrac{m_A E_R}{\mu_A} + \delta \right)$
- Similar energy spectrum from inelastic scatterings.

GUT embedding

Y. Abe, TT, K. Tsumura, N. Yamatsu, PRD (2021) [arXiv:2104.13523]

		fermions	H	S	Φ	~~SO(10)~~
	A_μ	Ψ_{16}	Φ_{10}	Φ_{16}	$\Phi_{\overline{126}}$	Φ_{210}
$SO(10)$	**45**	**16**	**10**	**16**	$\overline{\mathbf{126}}$	**210**

- We embed the UV complete model in SO(10) GUT.
- The pNGB model is reproduced at low energy.
- Breaking pattern: $SO(10) \;\to\; G_{\rm PS} \;\to\; G_{\rm SM}$

  at $\mu = M_U$ at $\mu = M_I$

  Pati-Salam symmetry: $G_{\rm PS} = SU(4)_C \times SU(2)_L \times SU(2)_R$
- GUT scale (M_U)
  Intermediate scale (M_I) = breaking scale of $U(1)_{B-L}$,
  Determined by matching conditions of gauge couplings

GUT embedding

Y. Abe, TT, K. Tsumura, N. Yamatsu, PRD (2021) [arXiv:2104.13523]

		fermions	H	S	Φ	~~SO(10)~~
	A_μ	Ψ_{16}	Φ_{10}	Φ_{16}	$\Phi_{\overline{126}}$	Φ_{210}
$SO(10)$	**45**	**16**	**10**	**16**	$\overline{\mathbf{126}}$	**210**

- Two U(1): $U(1)_{B-L} \subset SU(4)_C/SU(3)_C, \quad U(1)_R \subset SU(2)_R$
- $U(1)_{B-L}$ and $U(1)_R$ are orthogonal, but $U(1)_{B-L}$ and $U(1)_Y$ are not.

$$\begin{matrix} U(1)_Y \\ U(1)_{B-L} \end{matrix} : \begin{pmatrix} B_\mu \\ C_\mu \end{pmatrix} = \begin{pmatrix} 1 & -\tan\epsilon \\ 0 & \frac{1}{\cos\epsilon} \end{pmatrix} \begin{pmatrix} B'_\mu \\ C'_\mu \end{pmatrix} =: U_{GK} \begin{pmatrix} B'_\mu \\ C'_\mu \end{pmatrix} : \begin{matrix} U(1)_R \\ U(1)_{B-L} \end{matrix}$$

$\rightarrow$ Kinetic mixing between $U(1)_{B-L}$ and $U(1)_Y$: $\tan\epsilon = -\sqrt{2/3}$

- Proton decay
  SK limit: $\tau_{p\to e^+\pi^0} > 2.4\times10^{34}$ years
  Rough estimate: $\tau \sim (\alpha_U^2 m_p^5/M_U^4)^{-1} = 1.1\times10^{37}$ years

RGE

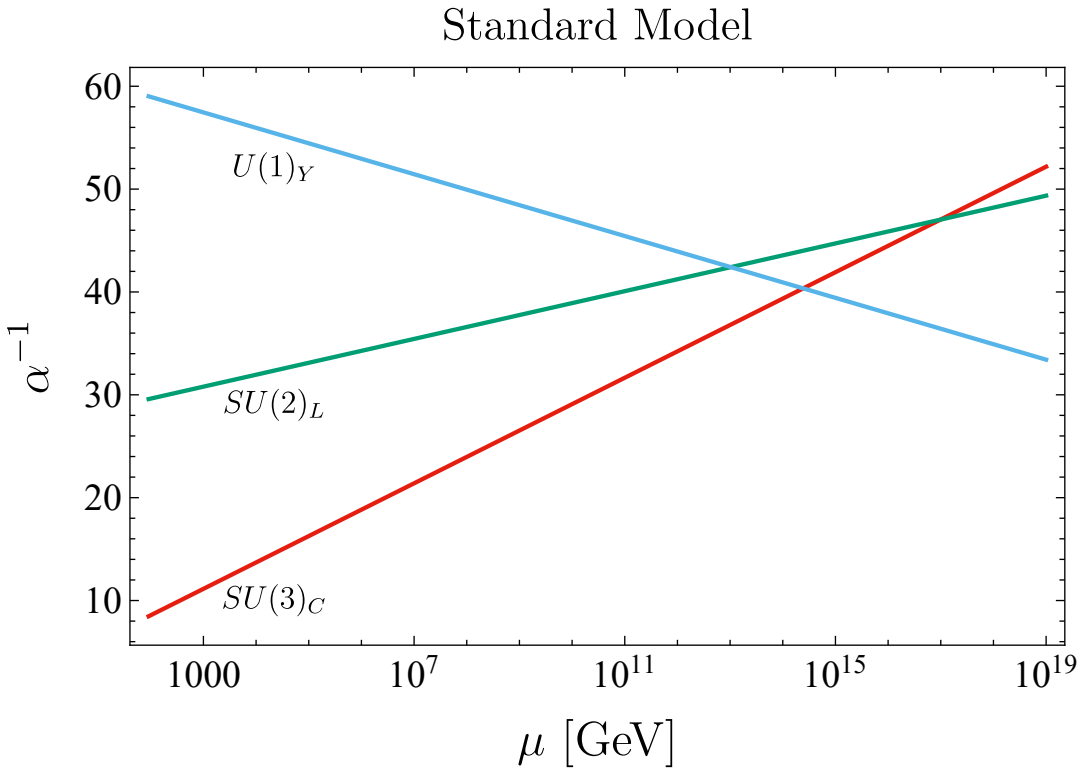

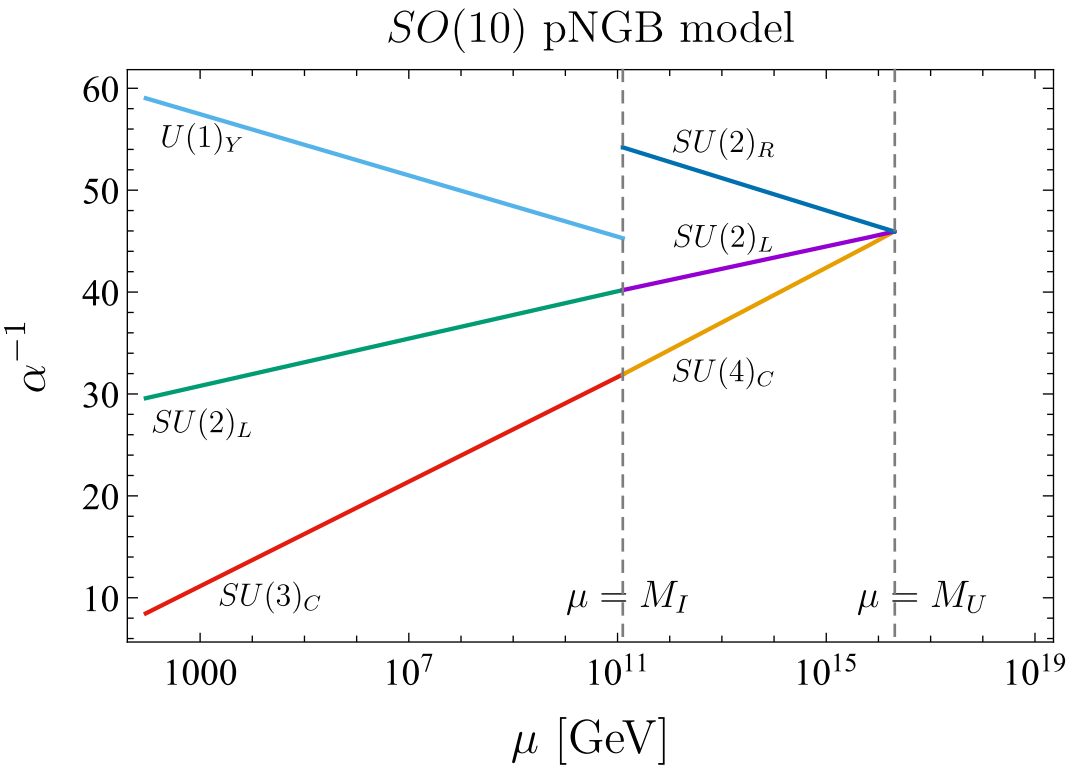

- 1-loop RGEs are solved.
- Intermediate scale, GUT scale: determined by matching conditions of gauge couplings
- $v_\phi = M_I = 1.26 \times 10^{11}$ GeV, $M_U = 2.06 \times 10^{16}$ GeV
  $g_{B-L} = 0.38$ at $\mu = M_I$

DM decay

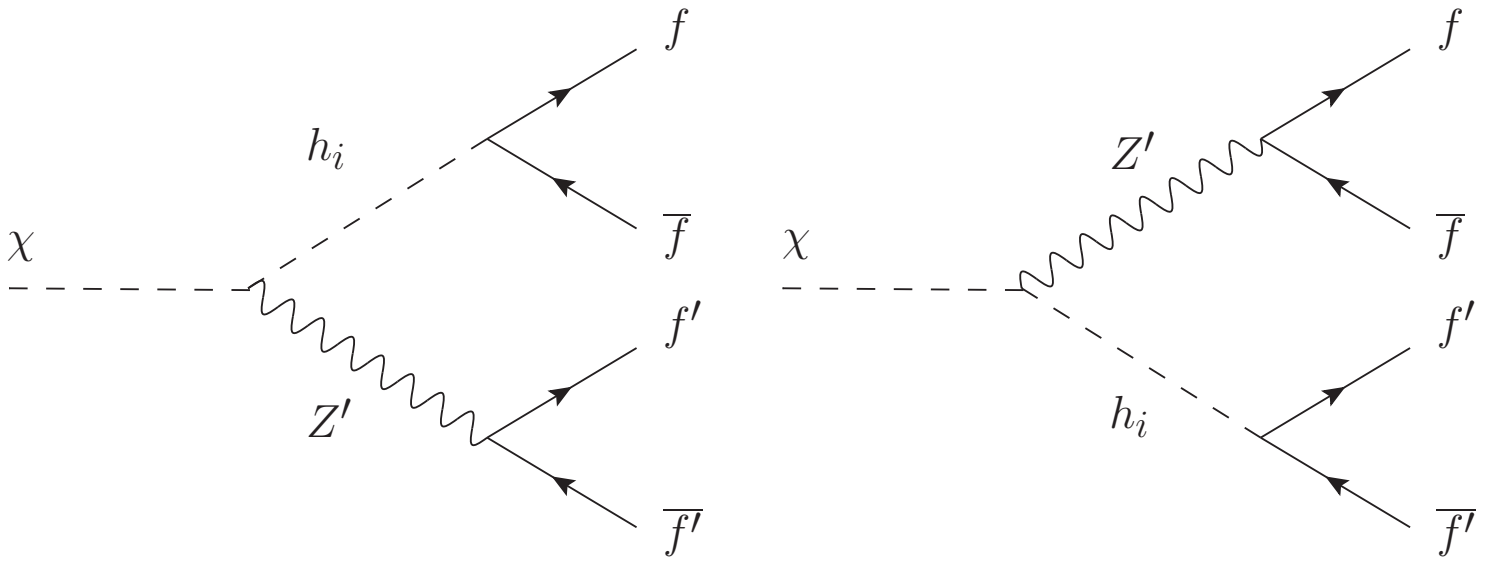

- DM lifetime: $\tau_{\rm DM} \gtrsim 10^{17}$ sec at least (the age of the universe).
- Cosmic ray observations give stronger limits: $\tau_{\rm DM} \gtrsim 10^{27}$ sec.
  3-body decays $\chi \to f\overline{f}h_i, f\overline{f}Z$ if $m_\chi \gtrsim m_{h_i}, m_Z \to$ excluded

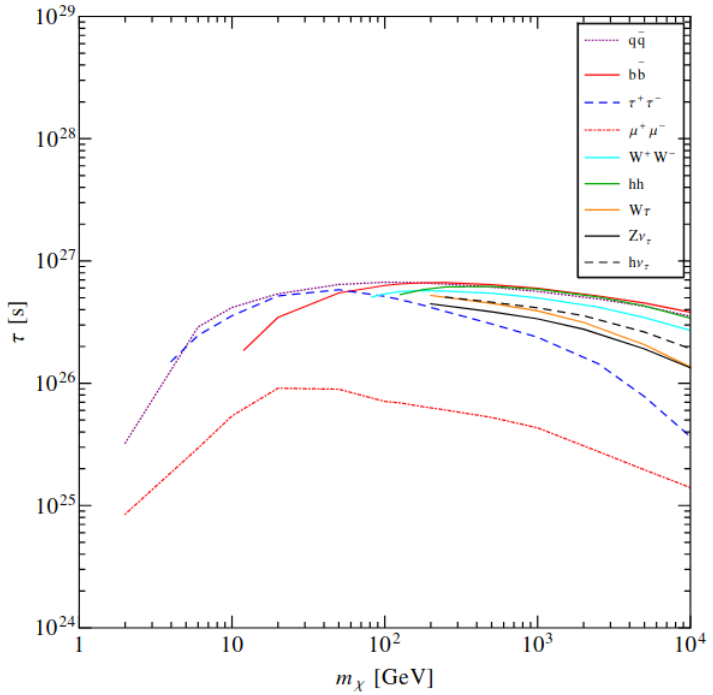

Baring et al. (2015)

DM decay2

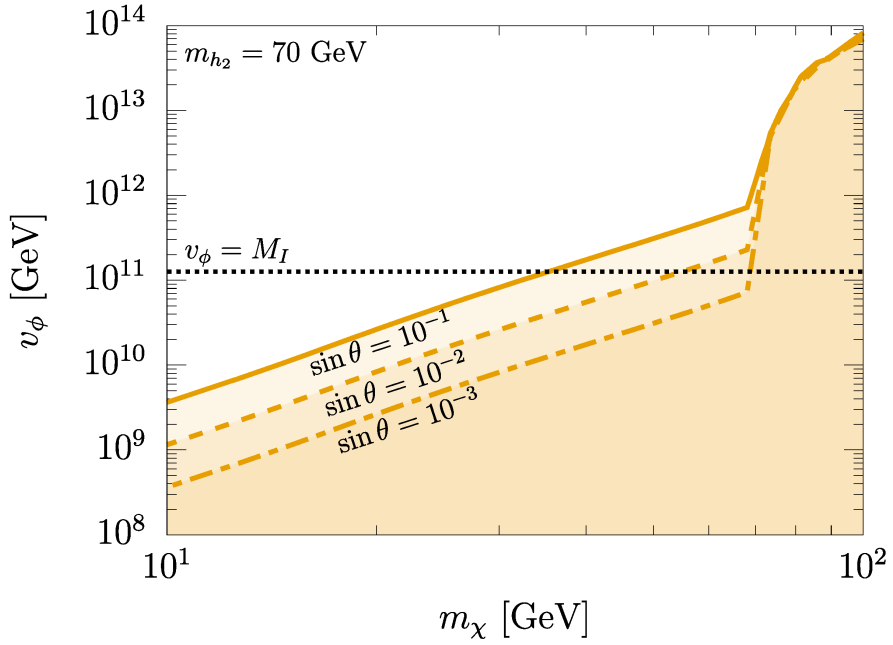

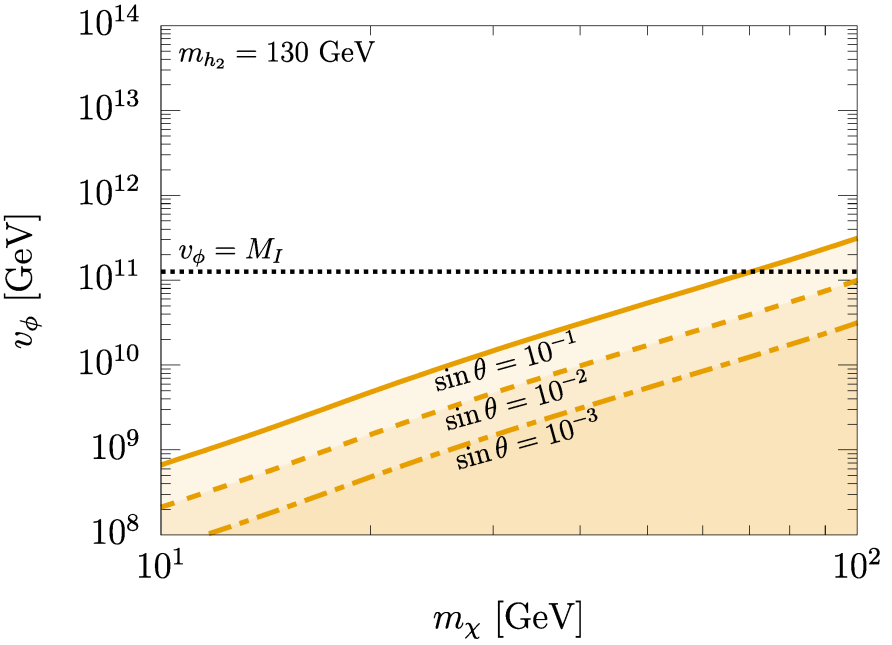

- Orange region is excluded. ($\tau_{\rm DM} \lesssim 10^{27}$ sec)
- DM should be $\lesssim 100$ GeV
- $v_\phi = M_I \sim 10^{11}$ GeV

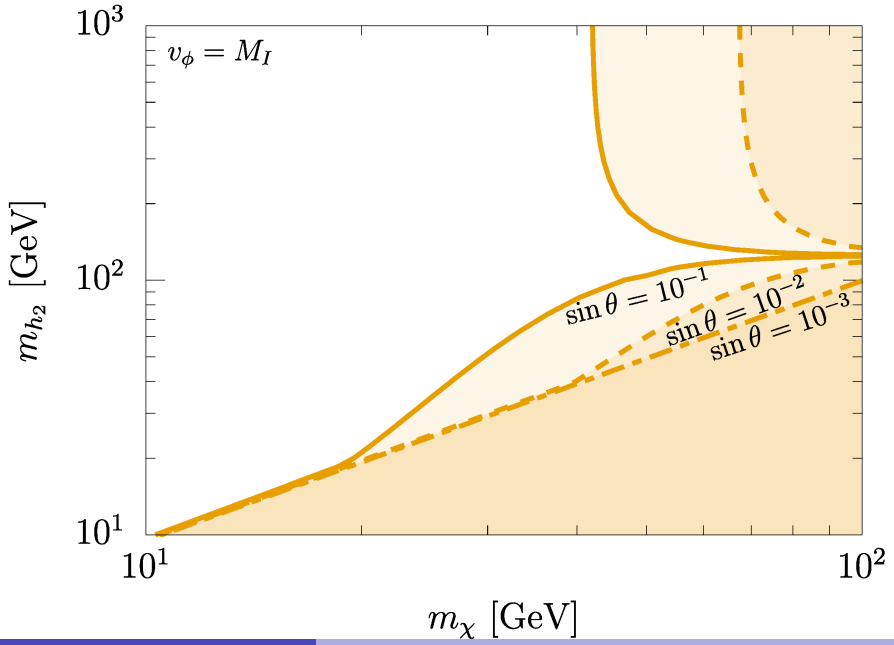

Parameter space

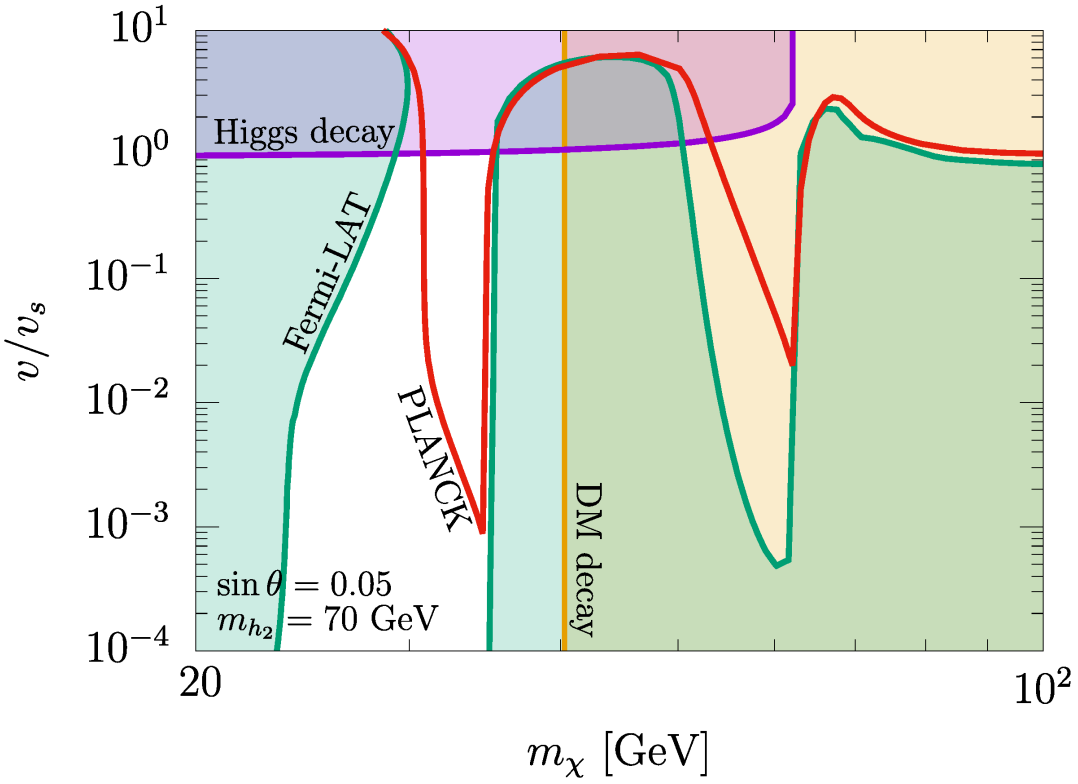

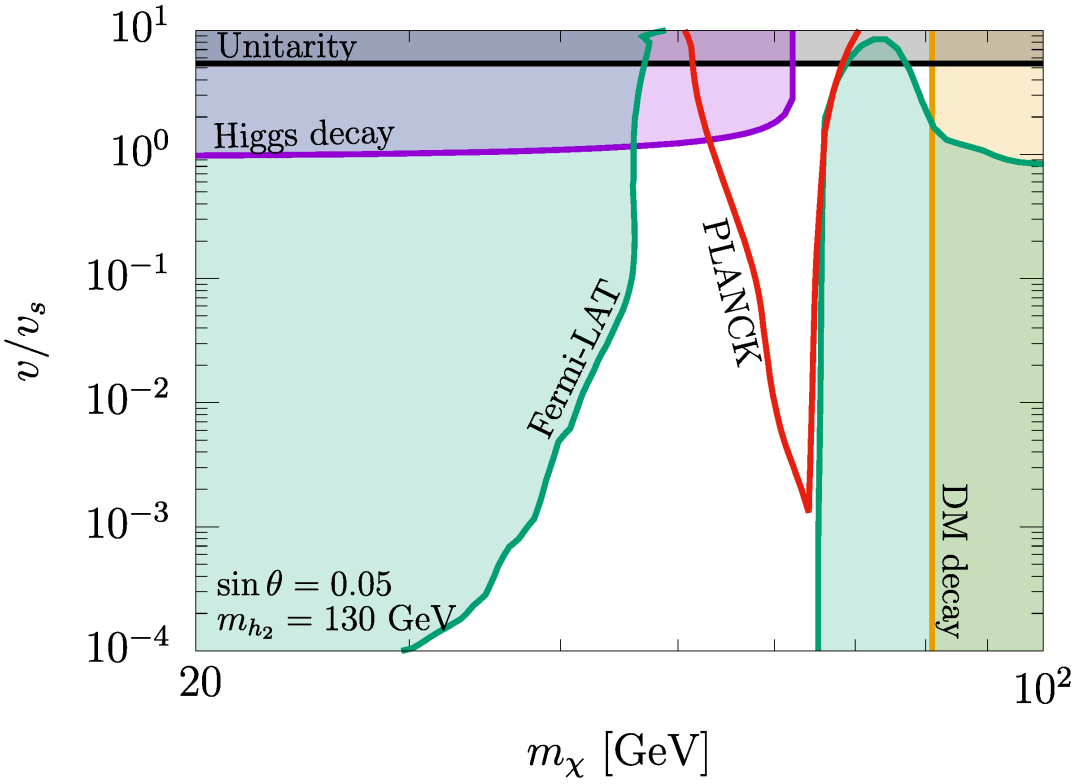

- $v/v_s \sim \sqrt{\lambda_S}$
- Fermi-LAT: $\chi\chi \to b\bar{b}, WW \to \gamma$ production
- close to the h_2 resonance

Indirect detection

DM annihilations

$\chi\chi \to h_i h_j, WW, ZZ, f\overline{f}$

- Gamma-rays are produced at the end
- Constraints from dSphs
  (less visible matter and more DM)

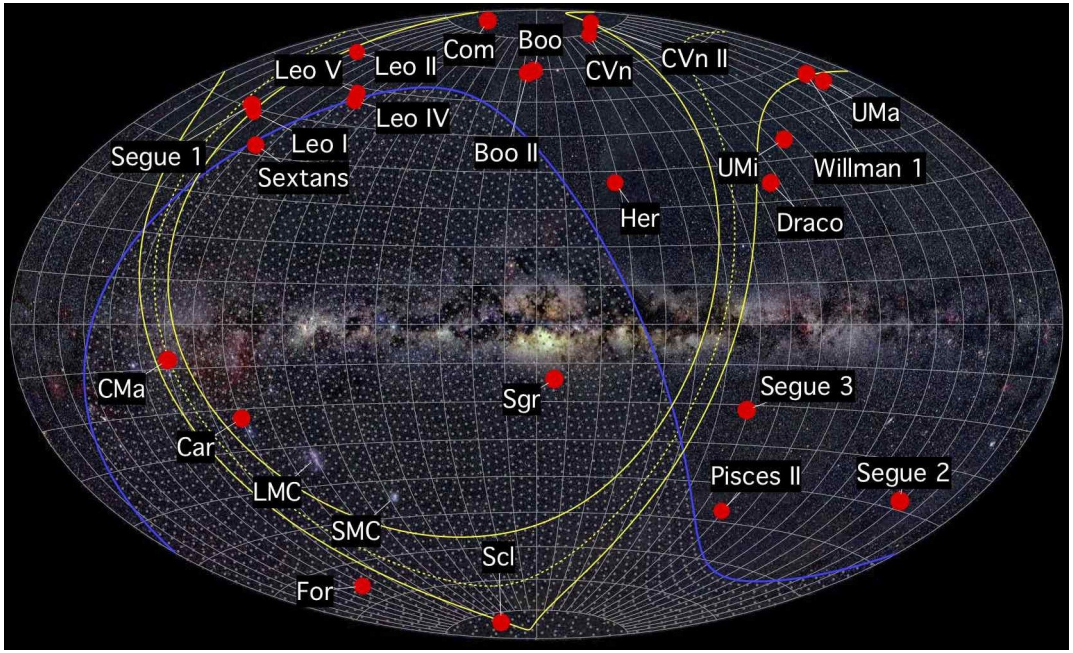

©A. Frebel (MIT)

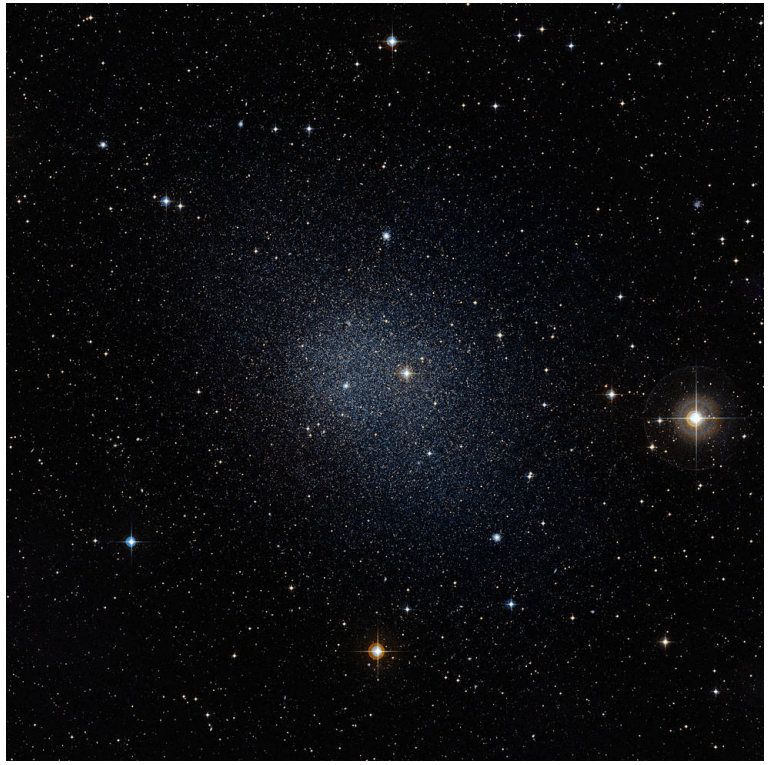

- $\mathcal{O}(50)$ dSphs have been found so far.
- DM models are constrained.

Indirect detection

- Present bounds and future prospects ($\chi\chi \to b\bar{b}$)

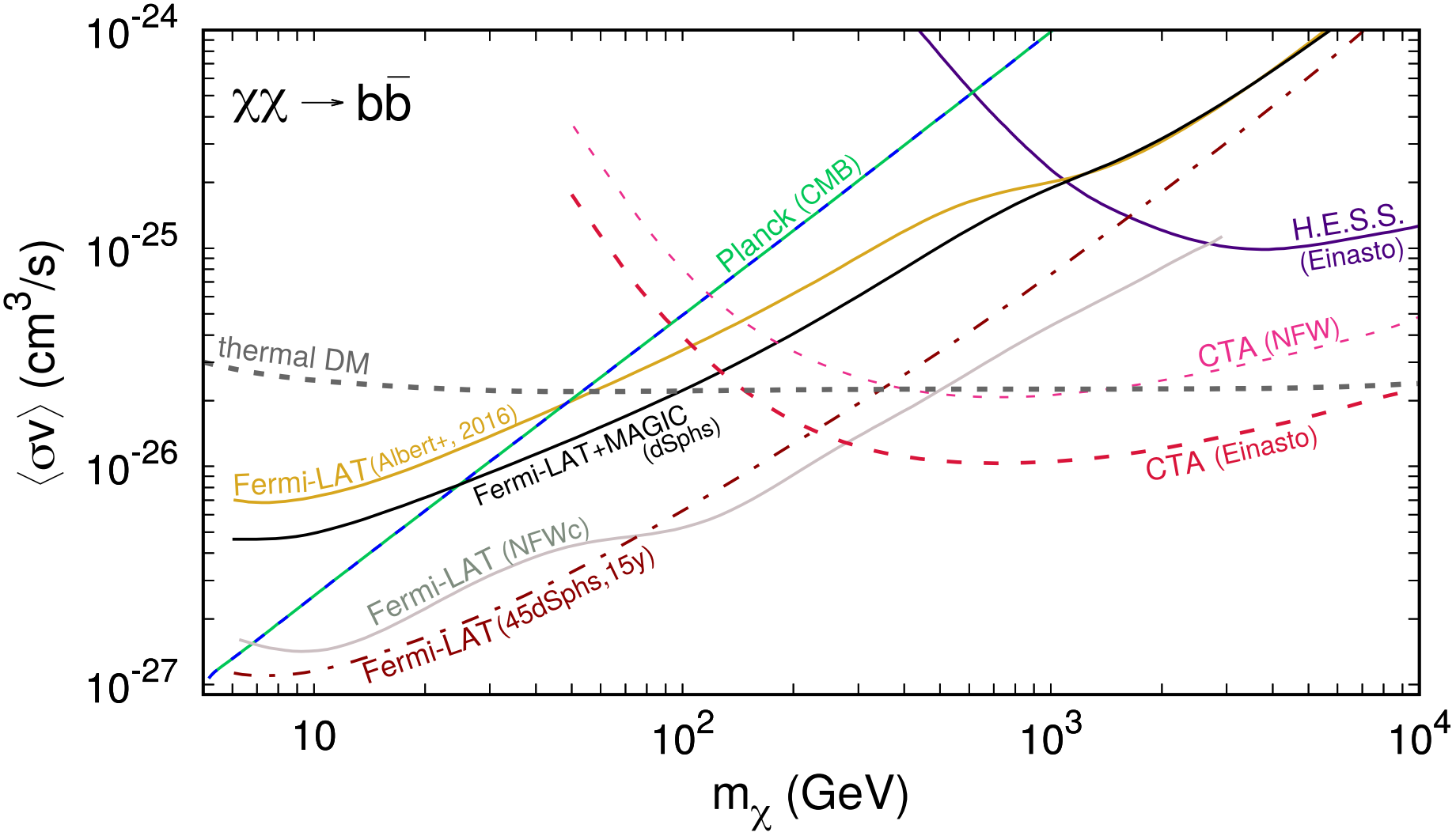

L. Roszkowski et al., Rept.Prog.Phys. 81 (2018), [arXiv:1707.06277]

Indirect detection

Huitu, Koivunen, Lebedev, Mondal, TT, arXiv:1812.05952

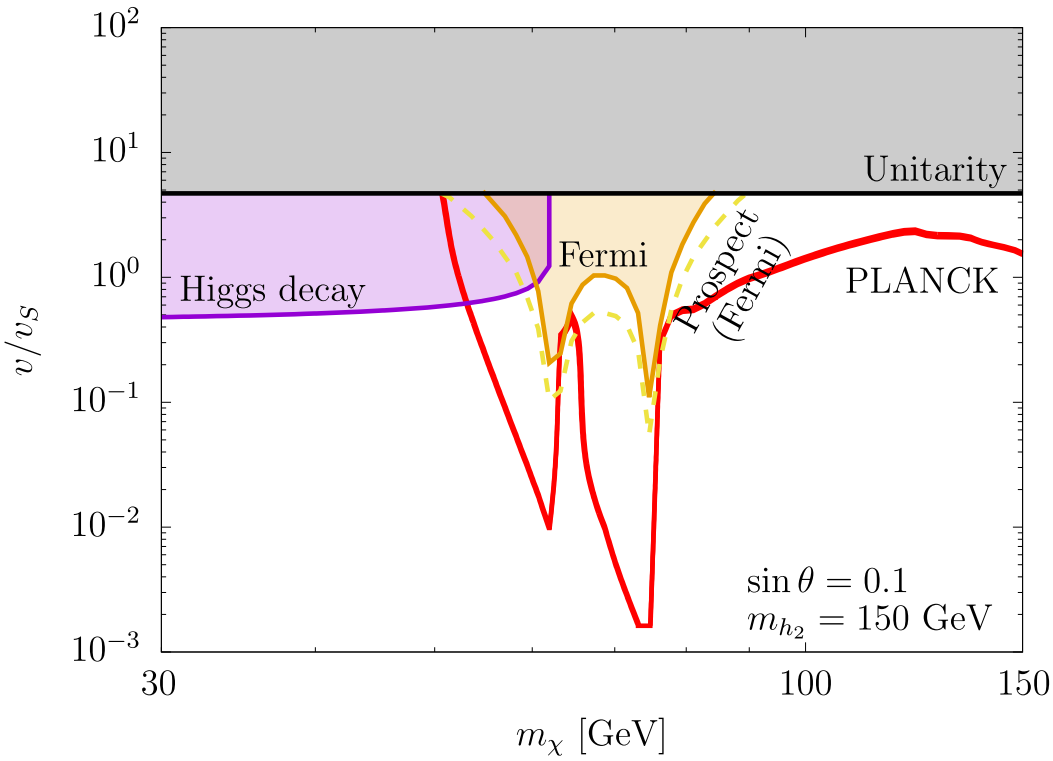

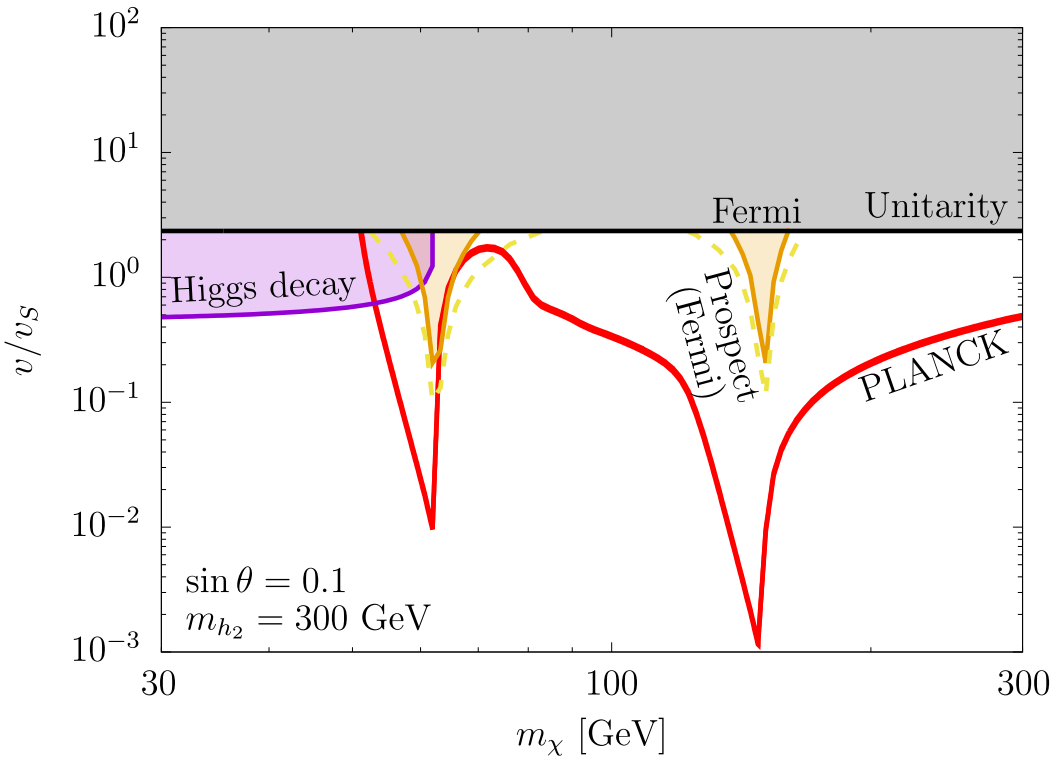

- Small parameter space is excluded by Fermi-LAT gamma-ray observation
- Thermal WIMP scenarios can be tested only when $m_\chi = \mathcal{O}(100)$ GeV
- CTA is sensitive in heavy DM mass region (DM profile dependent) ($\chi\chi \to h_2 h_2$ may dominate in this mass range)

Collider search

Huitu, Koivunen, Lebedev, Mondal, TT, PRD (2019) [arXiv:1812.05952]

- Constraint on h_2 production cross section at LHC

$$\sigma_{\rm prod} = \sigma(pp \to h_2)\ {\rm Br}(h_2 \to {\rm SM}) \quad \propto \quad \sin^2\theta\ {\rm Br}(h_2 \to {\rm SM})$$

- $pp \to h_2 \to ZZ$ mode
  When $\sin\theta \gtrsim 0.2$ and $m_{h_2} \lesssim 2m_{h_1}$, parameters are constrained.

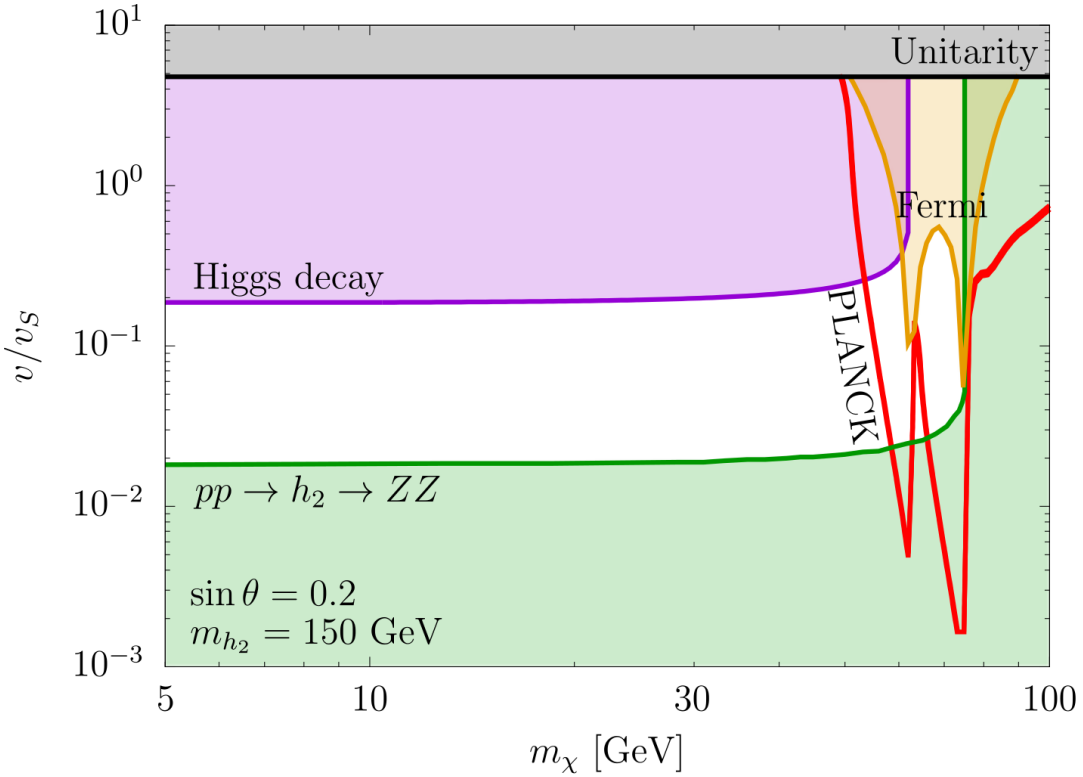

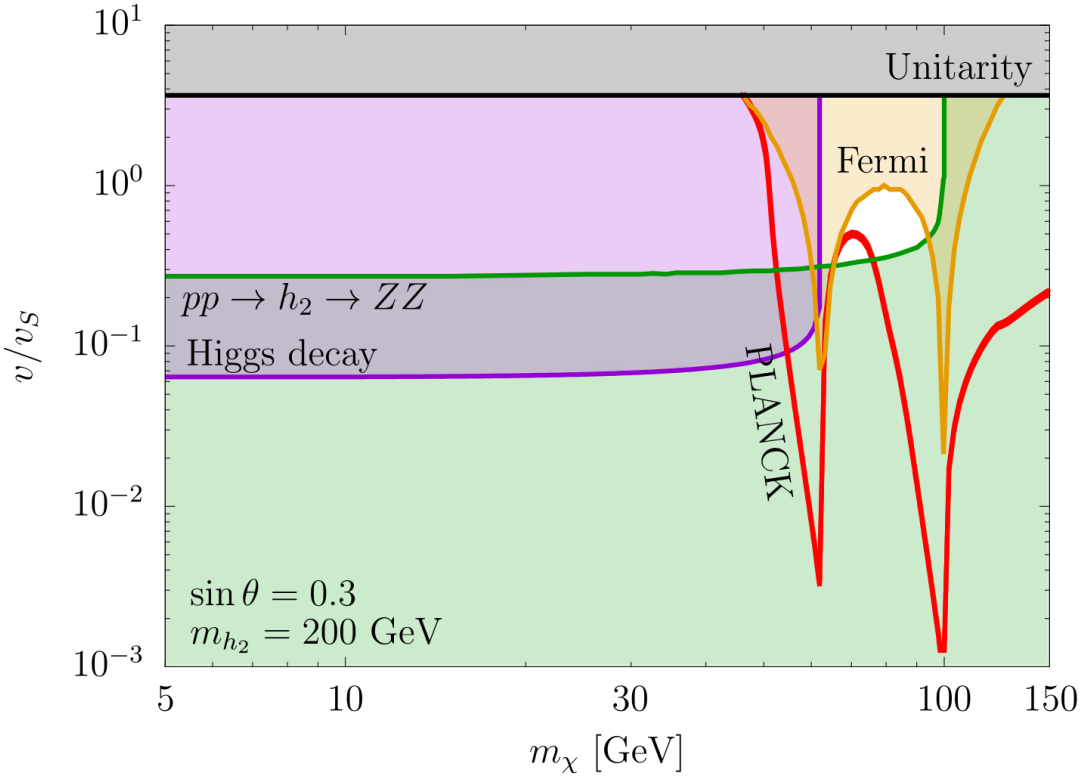

Collider search

Huitu, Koivunen, Lebedev, Mondal, TT, PRD (2019) [arXiv:1812.05952]

- Signal channel (VBF)
  h_1 and h_2, both contributions are important
- We focus on $m_{h_2} \geq 2m_\chi$
- Simulate the events and put appropriate cuts
  $\not{E}_T > 250$ GeV, $p_j > 80$ GeV etc

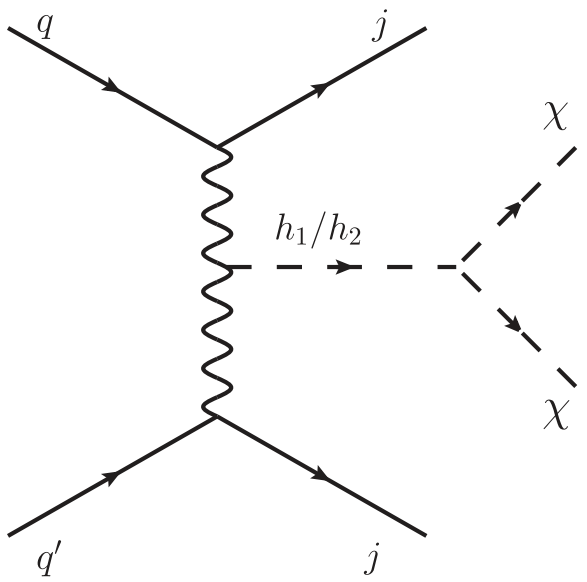

- Signal significance $\mathcal{S} = \dfrac{S}{\sqrt{S + B + \sigma_B^2}}$
- Background $B \pm \sigma_B = 1779 \pm 96$ at $35.9\ \mathrm{fb}^{-1}$ (CMS)
- Analyzed with $3000\ \mathrm{fb}^{-1}$.

Collider search

Huitu, Koivunen, Lebedev, Mondal, TT, PRD (2019) [arXiv:1812.05952]

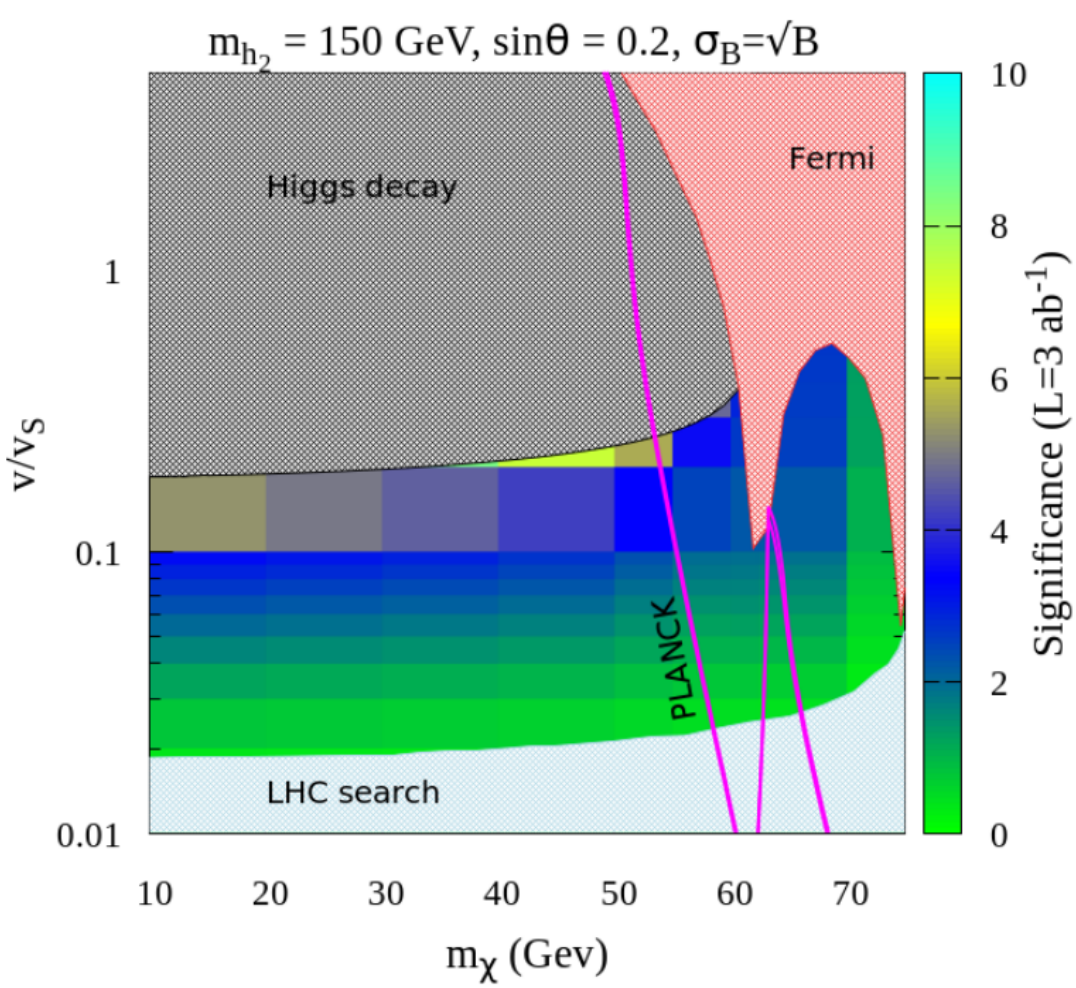

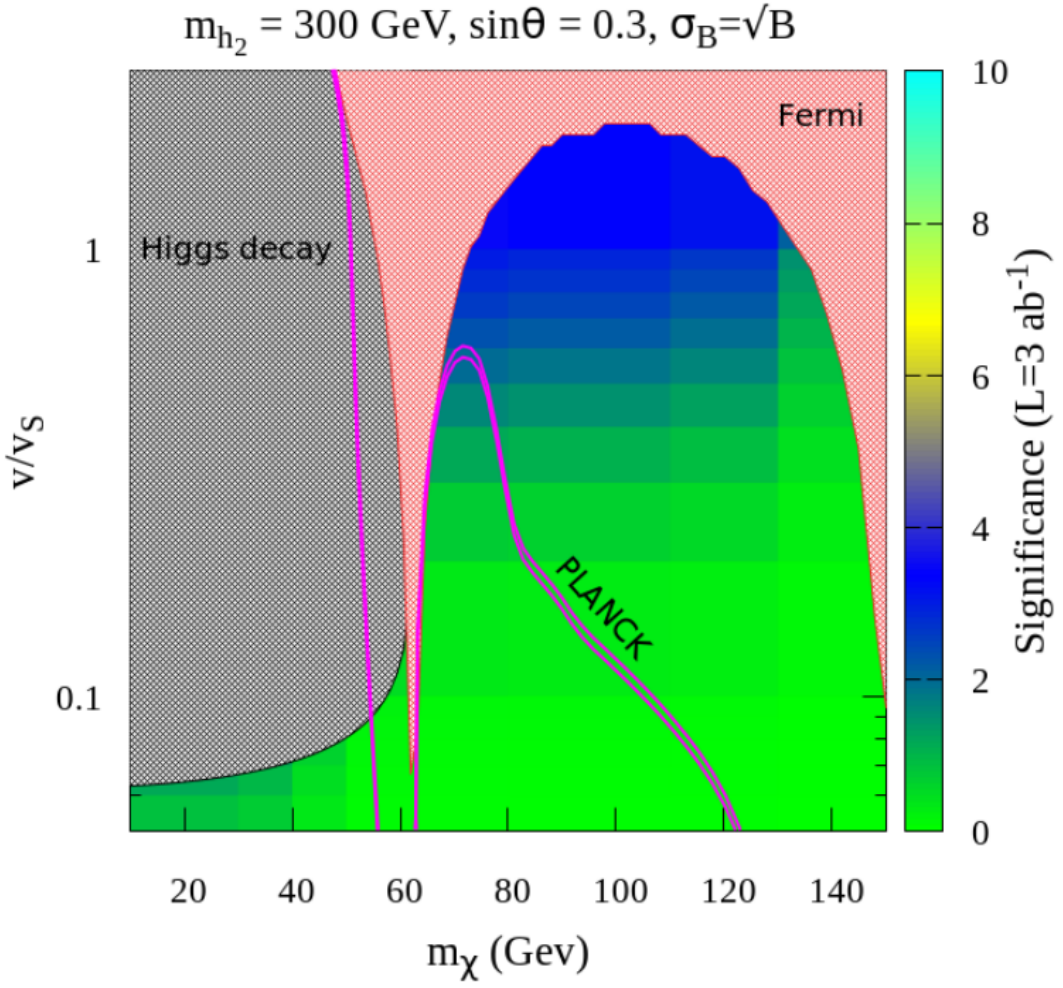

- Signal significance can be $\mathcal{S} \approx 4 - 6$ at most.
- $m_\chi \lesssim 100$ GeV can be visible.

Direct detection (1-loop level) K. Ishiwata, TT, JHEP [arXiv:1810.08139]

- Compute Feynman diagrams at 1-loop level

$$\sigma_{\rm SI}^N = \frac{1}{\pi}\frac{m_N^2}{(m_\chi + m_N)^2}|f_{\rm scalar}^N|^2$$

where $\frac{f_{\rm scalar}^N}{m_N} = \sum_{q=u,d,s} C_S^q f_{Tq}^N - \frac{8}{9} C_S^G f_{Tg}^N$ (f_{Tq}^N, f_{TG}^N: nucleon matrix elements)

$$\langle N|m_q \bar{q} q|N\rangle = f_{Tq}^N m_N, \quad \langle N|\frac{\alpha_s}{\pi} G_{\mu\nu}^a G^{a\mu\nu}|N\rangle = -\frac{8}{9} f_{Tg}^N m_N$$

f_{Tq}^N, f_{Tg}^N are calculated by QCD lattice simulation

$$\mathcal{L}_{\rm eff} = C_S^q m_q \chi^2 \bar{q} q + C_S^G \frac{\alpha_s}{\pi} \chi^2 G_{\mu\nu}^a G^{a\mu\nu} \quad \leftarrow C_S^q \text{ and } C_S^G \text{ (calculated)}$$

- Calculate up to 2-loop level in terms of QCD α_s (NLO)
  $\rightarrow$ scattering amplitude is $\mathcal{O}(\alpha_s)$ J. Hisano, K. Ishiwata, N. Nagata, arXiv:1504.00915

Direct detection (1-loop level)

K. Ishiwata, TT, JHEP [arXiv:1810.08139]

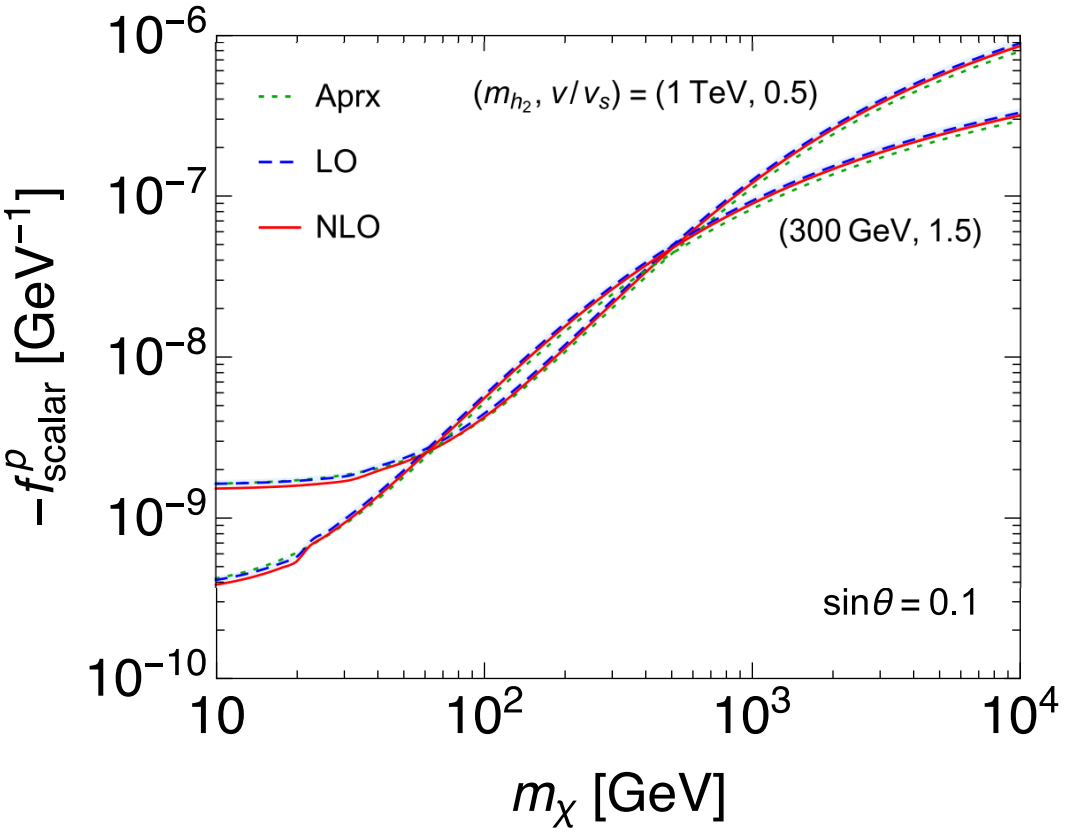

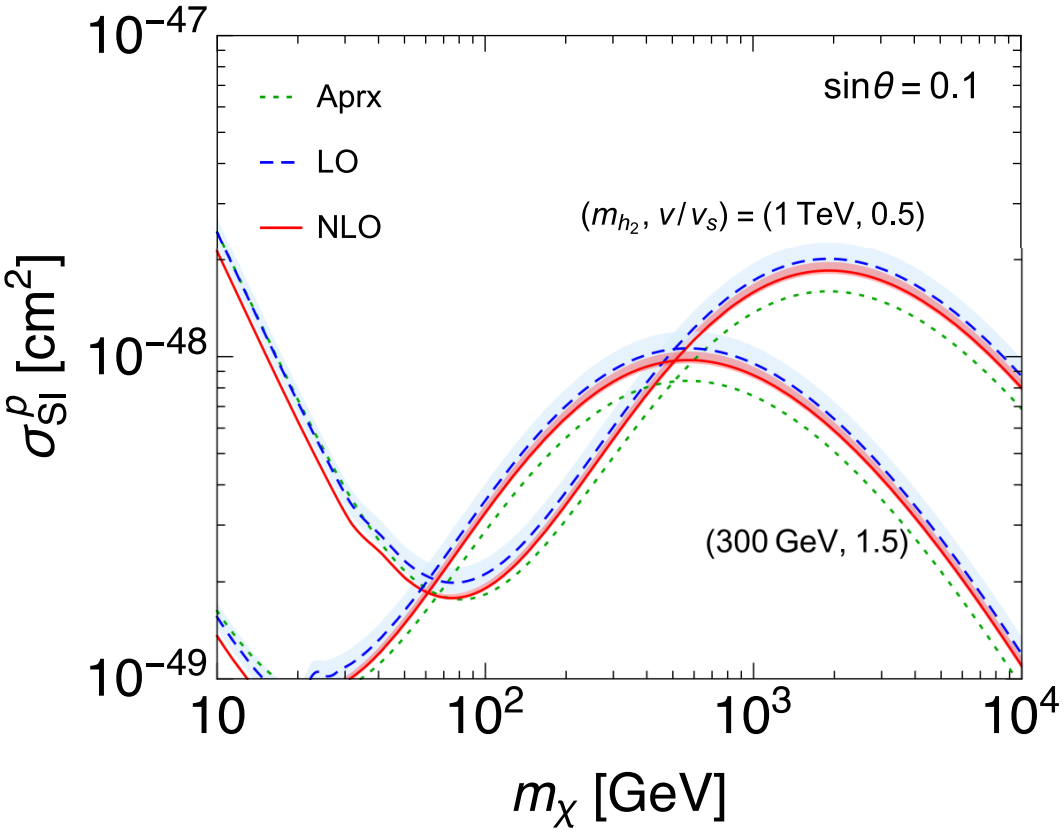

- (i)+(ii) is dominant for large DM mass
- NLO is $\mathcal{O}(10\%)$ correction

Origin of the soft term

C. Gross, O. Lebedev, TT, PRL (2017) [arXiv:1708.02253]

- $U(1)$ is extended to gauge symmetry, and a new field Φ is introduced
- Odd charge for S, even charge for Φ
  Ex. $q_S = 3$, $q_\Phi = 2$

$$\mathcal{V} \supset \frac{1}{\Lambda}\Phi^{\dagger 3}S^2 + \frac{1}{\Lambda^3}\Phi^{\dagger 3}|H|^2S^2 + \frac{1}{\Lambda^3}\Phi^{\dagger 3}|S|^2S^2 + \cdots$$

- After Φ gets a VEV, μ'_S is generated ($\mu'^2_S = \langle\Phi\rangle^3/\Lambda$)
- Other terms are suppressed by higher dimensional operators
  $\rightarrow$ the previous model is reproduced in low energy

- CP violation induces DM decay

$$\mathcal{V} \supset \left(\frac{\langle\Phi\rangle}{\Lambda}\right)^3 |H|^2 s\chi \quad \rightarrow \text{lifetime } \tau_\chi \sim \frac{8\pi}{100\ \text{GeV}}\left(\frac{\Lambda}{\langle\Phi\rangle}\right)^6$$

Ex. when $\Lambda = 10^{16}$ GeV, $\langle\Phi\rangle = 10^7$ GeV $\Rightarrow \tau_\chi \sim 10^{29}$ s

Collider anomalies

Heinemeyer, Stefaniak, arXiv:1812.05864
CMS-PAS-HIG-14-037, CMS-PAS-HIG-17-013

- Collider anomalies around $96\ \mathrm{GeV}$. 2.3σ (LEP) and 2.9σ (CMS)

$$b\bar{b}\text{ excess at LEP}: \quad \mu_{\rm LEP} \equiv \frac{\sigma_{\rm exp}(e^+e^- \to h_2 \to Zb\bar{b})}{\sigma_{\rm SM}(e^+e^- \to h_{\rm SM}(96) \to Zb\bar{b})} = 0.117 \pm 0.057$$

$$\gamma\gamma\text{ excess at CMS}: \quad \mu_{\rm CMS} \equiv \frac{\sigma_{\rm exp}(gg \to h_2 \to \gamma\gamma)}{\sigma_{\rm SM}(gg \to h_{\rm SM}(96) \to \gamma\gamma)} = 0.6 \pm 0.2$$

- Both anomalies cannot be explained at the same time in the model.
- But can be explained if a new scalar quark Φ is added.
  $\to$ chanage $h\gamma\gamma$ and hgg effective couplings (and other couplings)
- Φ is triplet or sextet

$$\mathcal{L} = -\lambda_{S\Phi}|S|^2|\Phi|^2 - \lambda_{H\Phi}|H|^2|\Phi|^2 + \left(y_\Phi \Phi^* \overline{q_R} q_R^c \quad \text{or} \quad \frac{\Phi}{\Lambda^3}\left(\overline{q_R} q_R^c\right)^2 \right)$$

$$m_\Phi^2 = \mu_\Phi^2 + \frac{\lambda_{S\Phi}}{2} v_s^2 + \frac{\lambda_{H\Phi}}{2} v^2 \equiv \mu_\Phi^2 + \overline{\mu}_\Phi^2$$

Collider anomalies

Cline, TT, PRD (2019) [arXiv:1906.07659]

- Model list:

model	q_Φ	N_c	$\frac{m_\Phi}{\lvert\lambda_{S\Phi}\rvert^{1/2}}$ [GeV]	$\frac{\overline{\mu}_\Phi}{\lvert\lambda_{S\Phi}\rvert^{1/2}}$ [GeV]	s_θ	$\lambda_{S\Phi}$	$\lambda_{H\Phi}$	χ^2/d.o.f.
1	$8/3$	6	943	836	0.39	1.9	3.3	3.6
2	$8/3$	3	601	778	0.36	1.4	1.6	2.2
3	$5/3$	6	700	741	0.34	3.4	3.5	2.1
4	$5/3$	3	417	838	0.39	3.0	5.2	3.7
5	$2/3$	6	588	795	0.37	4.8	5.9	1.4
6(*)	$2/3$	3	284	765	0.35	3.4	3.6	1.5
7	$-1/3$	6	554	830	0.39	5.4	8.0	1.5
8(*)	$-1/3$	3	256	810	0.38	4.1	5.6	1.4
9	$-4/3$	6	666	752	0.35	3.8	3.9	1.8
10(*)	$-4/3$	3	333	737	0.34	2.4	3.0	2.5

- We need large couplings $\lambda_{S\Phi}$, $\lambda_{H\Phi}$, and large mixing s_θ
- Mass bounds: $m_\Phi \gtrsim 720$ GeV (triplet 4jet)
  $m_\Phi \gtrsim 1.3$ TeV (sextet 4jet)
  $m_\Phi \gtrsim 520$ GeV (triplet 2jet)

Collider anomalies

Cline, TT, PRD (2019) [arXiv:1906.07659]

- $\kappa_\gamma - \kappa_g$ plane

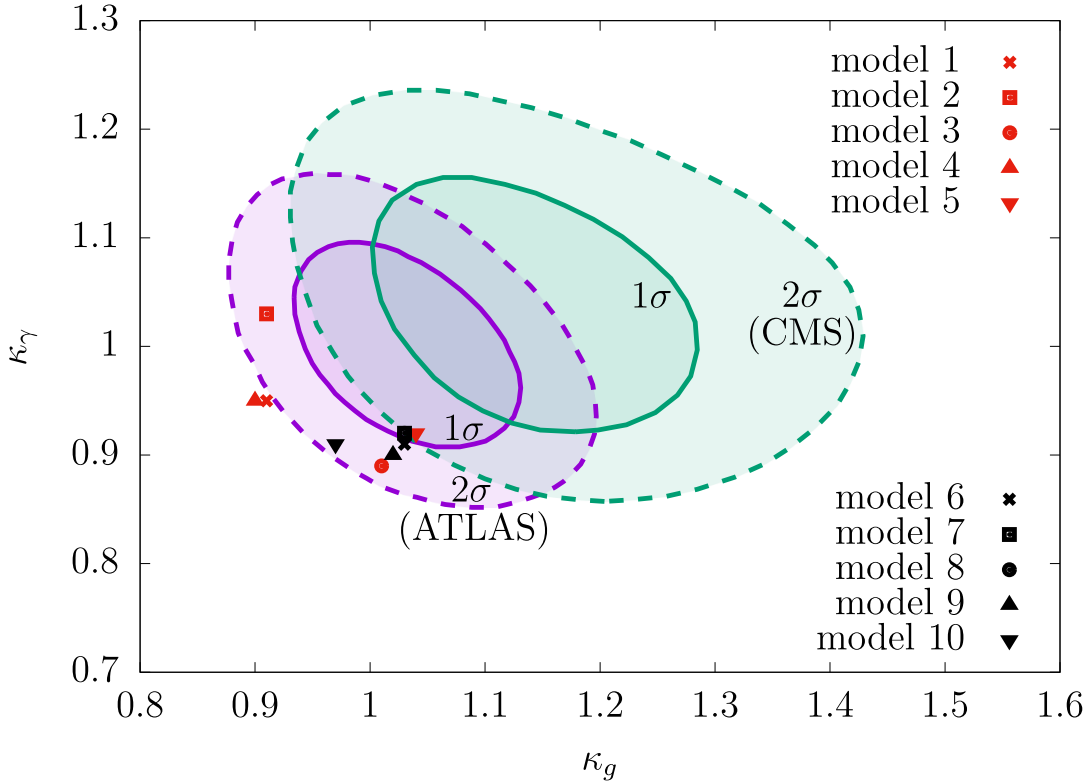

- Higgs couling strengths are also affected

$$\kappa_i = \frac{\text{coupling in our model}}{\text{coupling in SM}}$$

ex. $\mathcal{L} = g_{hZZ} h Z^2 \to \kappa_Z = c_\theta$

- Model 5,6,7,8 within 2σ range (all observables).

- $\chi\chi \to \gamma\gamma$ is also enhanced by Φ. $\to \sigma_{\gamma\gamma} v \sim 10^{-28}\ \mathrm{cm}^3/\mathrm{s}$ slightly below the Fermi bound $(0.5 - 4) \times 10^{-28}\ \mathrm{cm}^3/\mathrm{s}$

Cosmic ray anomalies

Cholis, Linden, Hooper, PRD (2019) [arXiv:1903.02549]

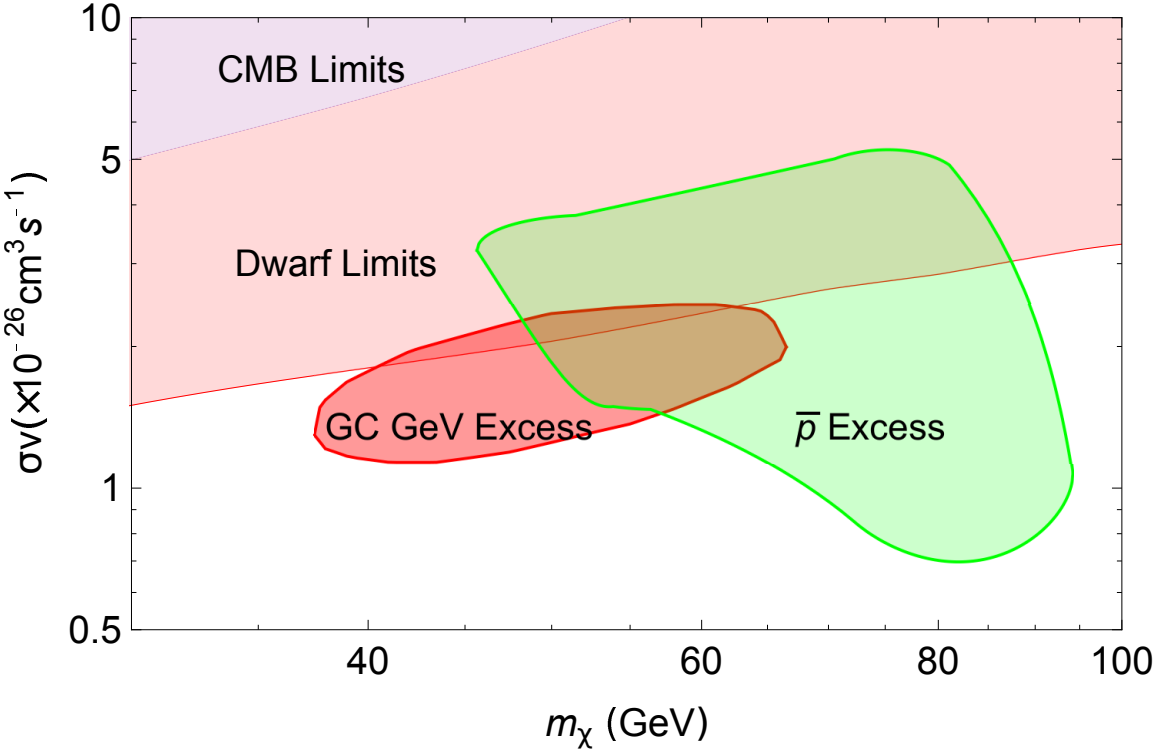

- Excesses in gamma ray and anti-proton cosmic ray. $\gtrsim 4\sigma$
- could be (thermal) DM signal. (other explanations: pulser etc)
  $\chi\chi \to f\overline{f}, WW, ZZ \to \gamma, \overline{p}$
- Cross section: $\langle \sigma_{b\bar{b}} v \rangle \approx (0.8 - 5.2) \times 10^{-26}\ \mathrm{cm}^3/\mathrm{s}$
  DM mass: $64 - 88\ \mathrm{GeV}$

$\to$ coincide with $\langle \sigma v \rangle$ for thermal WIMP scenarios.

- Typical thermal WIMP conflicts with direct detection bound.
  But pseudo Goldstone DM can naturally avoid the constraint.

Cosmic ray anomalies

Cline, TT, PRD (2019) [arXiv:1906.07659]

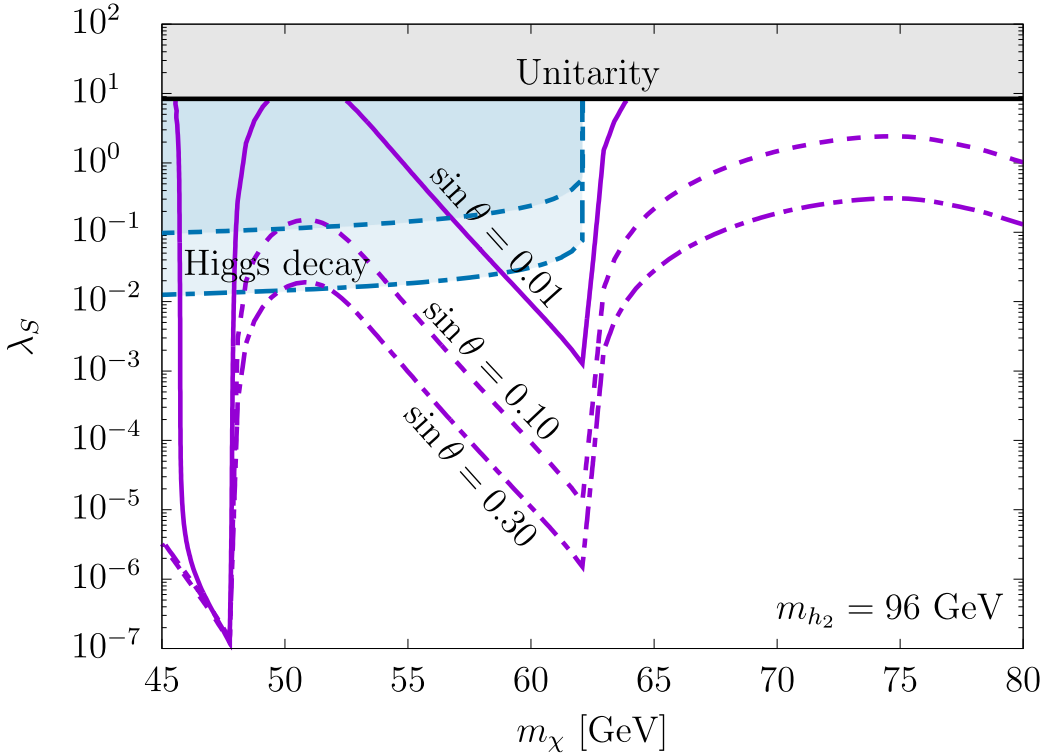

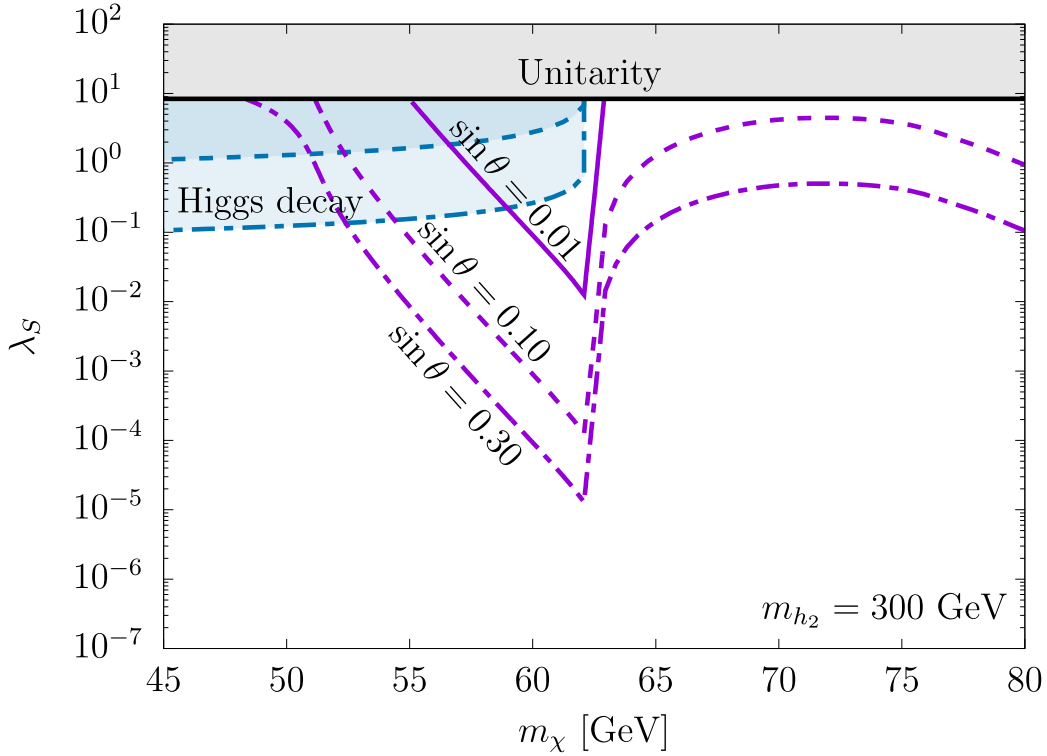

- $m_{h_2} = 96, 300$ GeV.
- Higgs invisible decay $\mathrm{Br}(h_1 \to \mathrm{inv}) \lesssim 0.2$. $\Gamma_{\mathrm{inv}} = \dfrac{\sin^2\theta m_{h_1}^3}{32\pi v_s^2}\sqrt{1-4\dfrac{m_\chi^2}{m_{h_1}^2}}$
- Purple lines: thermal relic abundance at PLANCK

Cosmic ray anomalies

Cline, TT, PRD (2019) [arXiv:1906.07659]

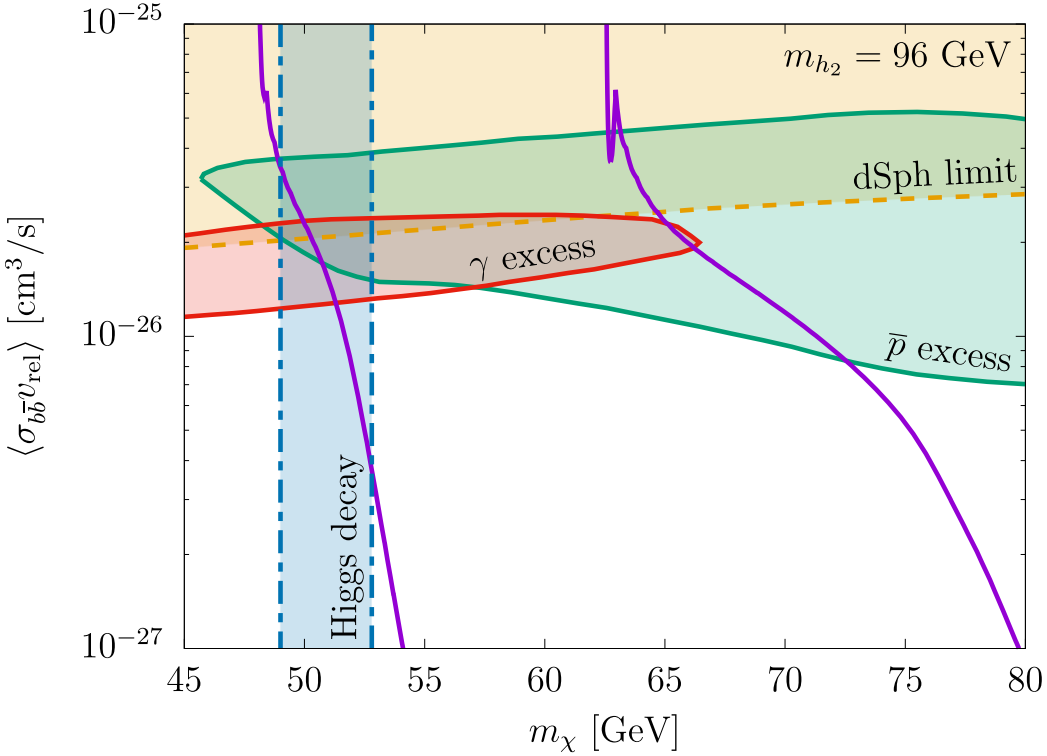

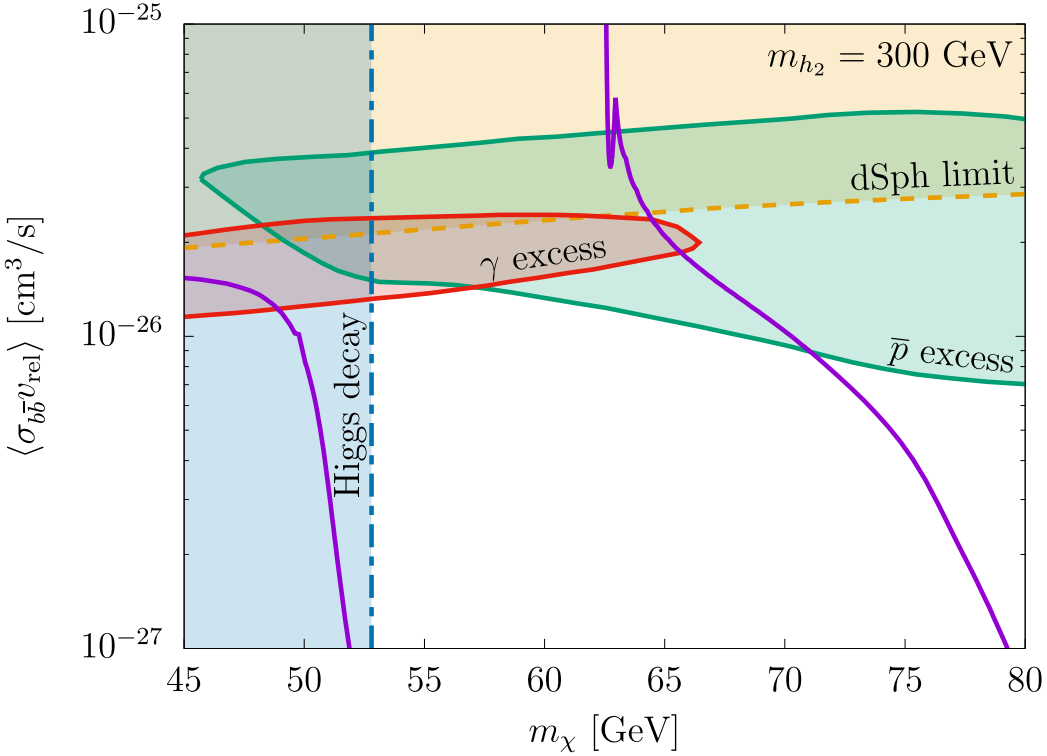

- $\chi\chi \to b\bar{b}$ cross section
- $m_{h_2} = 96, 300$ GeV.
- Additional channel $\chi\chi \to h_2 h_2$ if $m_\chi > m_{h_2}$. $\to$ mixing dependence
- Cosmic-ray anomalies can be explained by pseudo Goldstone DM in 2σ CL if $m_\chi = 64 - 67$ GeV.

Potential stability in SM

Degrassi et al., JHEP (2012) [arXiv:1205.6497]

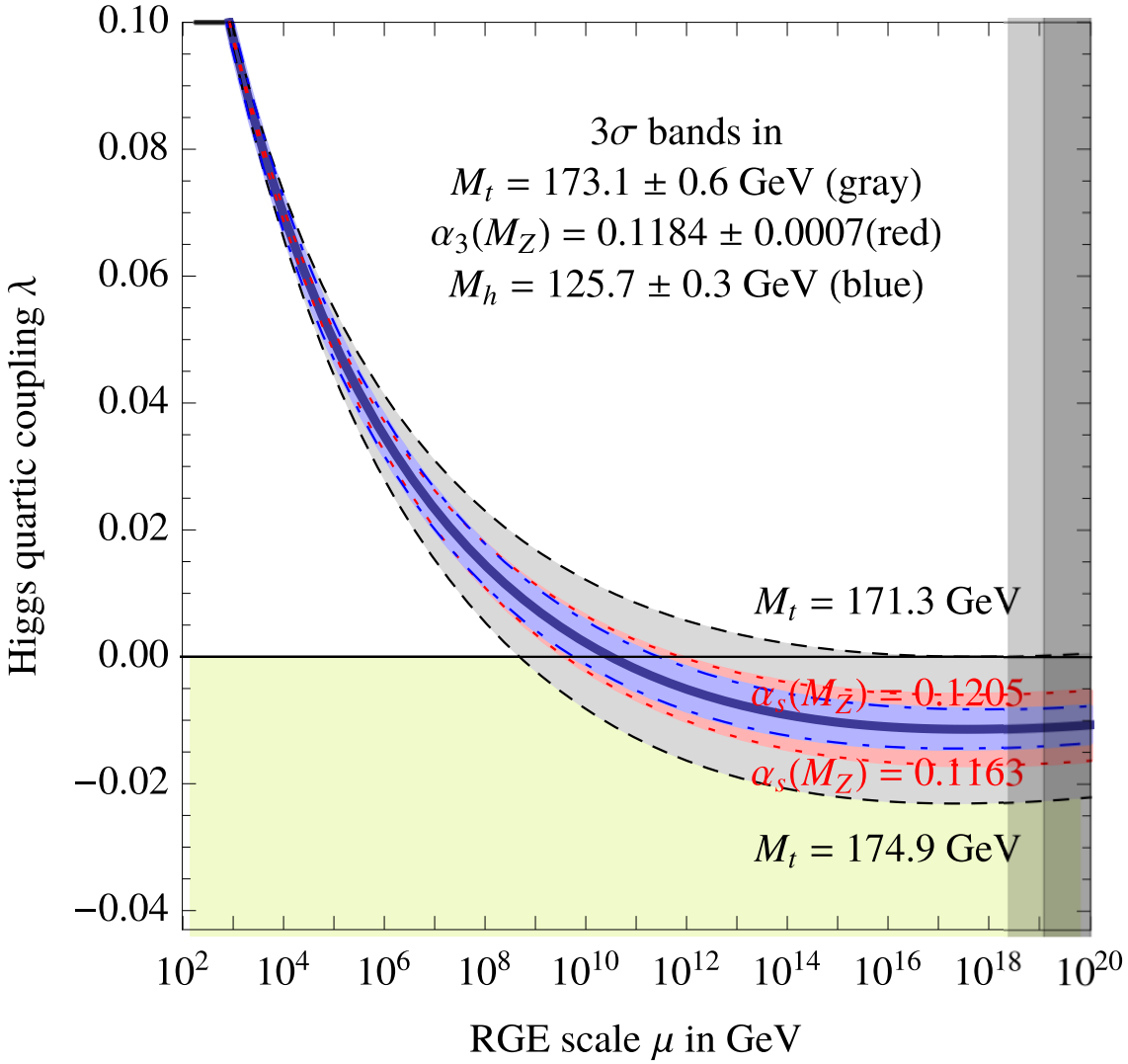

- Running of λ_H via β function
- Potential is destabilized around $\mu \sim 10^{11}$ GeV. $\rightarrow \lambda_H < 0$
- Strongly depends on m_t

Potential stability with h_2

Cline, TT, PRD (2019) [arXiv:1906.07659]

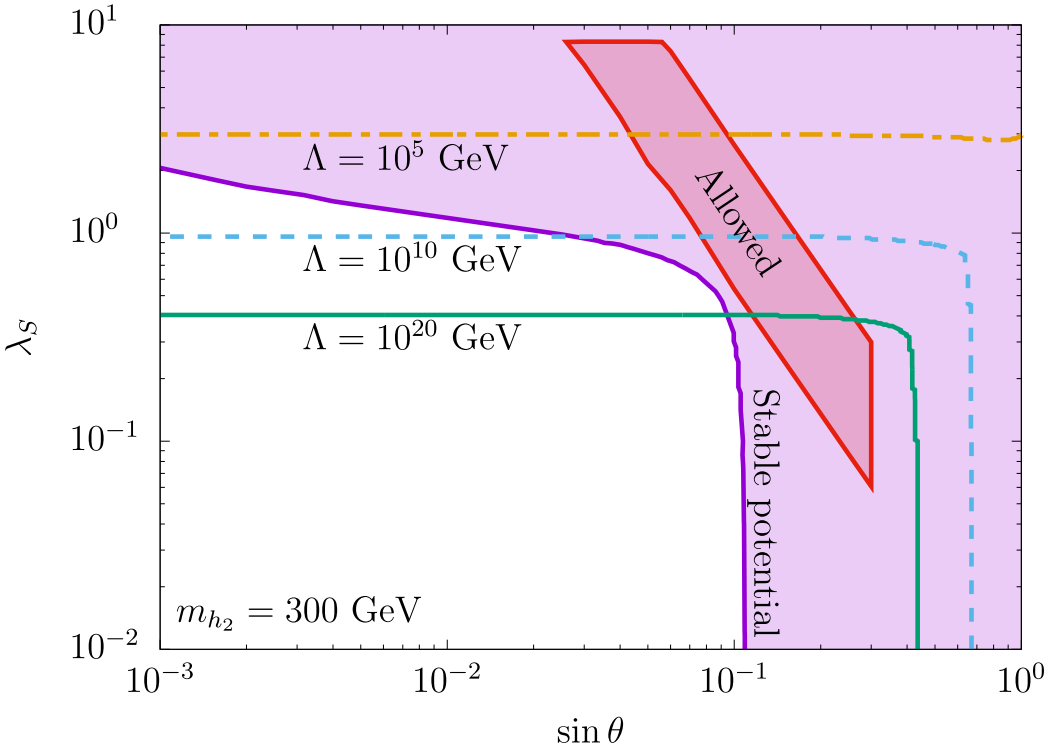

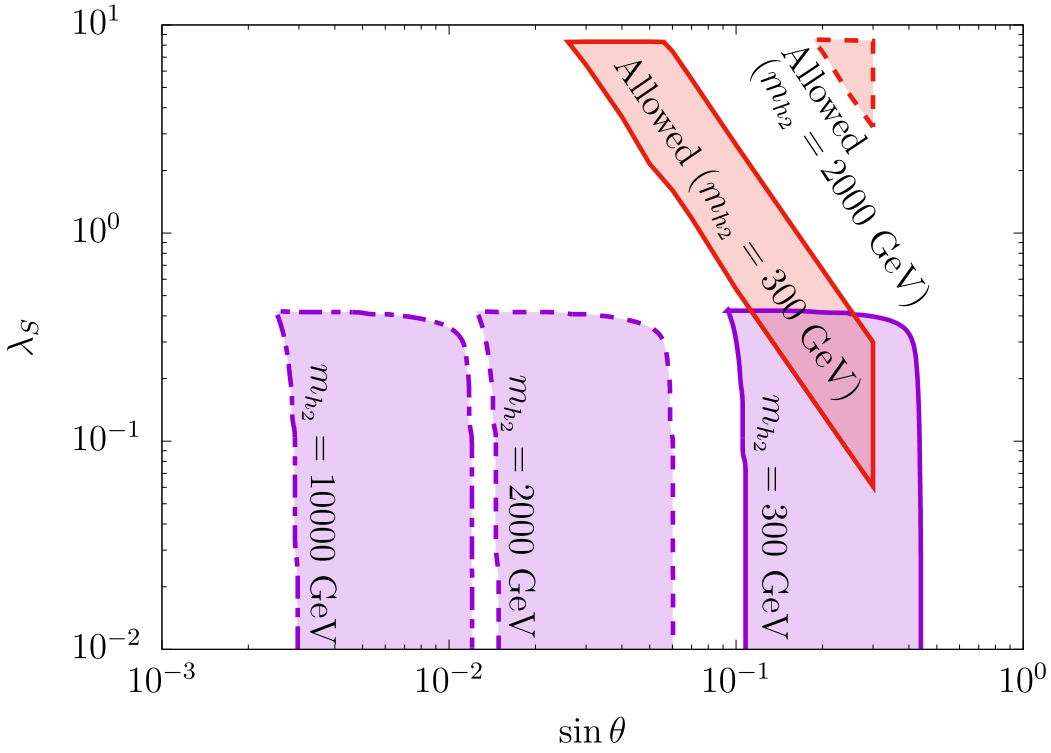

- Stability and perturbativity ($\leq 4\pi$) up to Planck scale
- Red region: explain cosmic ray anomalies
- Cosmic ray anomalies, potential stability and perturbative couplings up to Planck scale
  $\rightarrow 140 \lesssim m_{h_2} \lesssim 500$ GeV